TILLEGG 3

3. Some one-dimensional potentials

This "Tillegg" is a supplement to sections 3.1, 3.3 and 3.5 in Hemmer's book. Sections marked with *** are not part of the introductory courses (FY1006 and TFY4215).

3.1 General properties of energy eigenfunctions

(Hemmer 3.1, B&J 3.6)

For a particle moving in a one-dimensional potential $V(x)$, the energy eigenfunctions are the acceptable solutions of the time-independent Schrödinger equation $\widehat{H}\psi = E\psi$:

$$\left(-\frac{\hbar^2}{2m}\frac{\partial^2}{\partial x^2} + V(x)\right)\psi = E\psi, \qquad \text{or} \qquad \frac{d^2\psi}{dx^2} = \frac{2m}{\hbar^2}\left[V(x) - E\right]\psi. \tag{T3.1}$$

3.1.a Energy eigenfunctions can be chosen real

Locally, this second-order differential equation has two independent solutions. Since $V(x)$ and E both are real, we can notice that if a solution $\psi(x)$ (with energy E) of this equation is complex, then both the real and the imaginary parts of this solution,

$$\Re\mathrm{e}[\psi(x)] = \frac{1}{2}[\psi(x) + \psi^*(x)] \qquad \text{and} \qquad \Im\mathrm{m}[\psi(x)] = \frac{1}{2i}[\psi(x) - \psi^*(x)],$$

will satisfy (T3.1), for the energy E. This means that we can *choose* to work with two independent *real* solutions, if we wish (instead of the complex solutions $\psi(x)$ and $\psi^*(x)$). An example: For a free particle ($V(x) = 0$),

$$\psi(x) = e^{ikx}, \qquad \text{with} \quad k = \frac{1}{\hbar}\sqrt{2mE}$$

is a solution with energy E. But then also $\psi^*(x) = \exp(-ikx)$ is a solution with the same energy. If we wish, we can therefore choose to work with the real and imaginary parts of $\psi(x)$, which are respectively $\cos kx$ and $\sin kx$, cf particle in a box.

Working with real solutions is an advantage e.g. when we want to discuss curvature properties (cf section 3.1.c).

3.1.b Continuity properties [Hemmer 3.1, B&J 3.6]

(i) For a finite potential, $|V(x)| < \infty$, we see from (T3.1) that the second derivative of the wave function is everywhere finite. This means that $d\psi/dx$ and hence also ψ must be

continuous for all x:

$$\boxed{\frac{d\psi}{dx} \quad \text{and} \quad \psi(x) \quad \text{are continuous} \quad (\text{when} \quad |V(x)| < \infty).} \tag{T3.2}$$

This holds provided that the potential is finite, and therefore even if it is discontinuous, as in the examples

which show model potentials for a square well, a potential step and a barrier.

(ii) For a model potential $V(x)$ which is infinite in a region (e.g. inside a "hard wall"), it follows from (T3.1) that ψ must be equal to zero in this region. So here classical and quantum mechanics agree: The particle can not penetrate into the "hard wall". For such a potential, only the wave function ψ is continuous, while the derivative ψ' makes a jump. An example has already been encountered for the particle in a box:

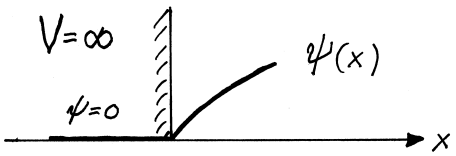

3.1.c Potentials with δ-function contributions

Some times we use model potentials with delta-function contributions (δ walls and/or barriers).

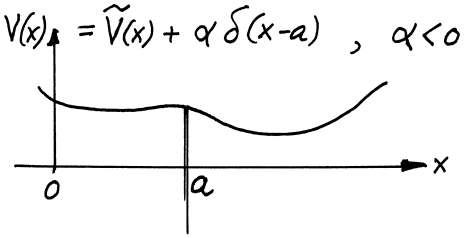

The figure shows a potential

$$V(x) = \widetilde{V}(x) + \alpha\delta(x-a) \qquad (\alpha < 0),$$

where $\widetilde{V}(x)$ is finite, with a delta-function well in addition, placed at $x = a$. We can now write (T3.1) on the form

$$\frac{d^2\psi}{dx^2} = \frac{2m}{\hbar^2}\left[\widetilde{V}(x) - E\right]\psi(x) + \frac{2m\alpha}{\hbar^2}\,\delta(x-a)\psi(x).$$

This equation can be integrated over a small interval containing the delta well:

$$\int_{a-\Delta}^{a+\Delta} \frac{d^2\psi}{dx^2} dx \;=\; \frac{2m}{\hbar^2} \int_{a-\Delta}^{a+\Delta} \left[\widetilde{V}(x) - E\right] \psi(x) dx + \frac{2m\alpha}{\hbar^2} \int_{a-\Delta}^{a+\Delta} \delta(x-a)\psi(x) dx,$$

or

$$\psi'(a+\Delta) - \psi'(a-\Delta) = \frac{2m}{\hbar^2} \int_{a-\Delta}^{a+\Delta} \left[\widetilde{V}(x) - E\right] \psi(x) dx + \frac{2m\alpha}{\hbar^2}\, \psi(a).$$

In the limit $\Delta \to 0$, the integral on the right becomes zero, giving the result

$$\boxed{\psi'(a^+) - \psi'(a^-) = \frac{2m\alpha}{\hbar^2}\, \psi(a)} \qquad \text{(T3.3)}$$

$$\text{when} \quad V(x) = \widetilde{V}(x) + \alpha\delta(x-a).$$

Equation (T3.3) shows that the derivative makes a jump at the point $x = a$, and that the size of this jump is proportional to the "strength" (α) of th δ-function potential, and also to the value $\psi(a)$ of the wave function at this point. (If the wave function happens to be equal to zero at the point $x = a$, we note that the wave function becomes smooth also at $x = a$.) Thus, at a point where the potential has a delta-function contribution, the derivative ψ' normally is *discontinuous*, while the wave function itself is continuous everywhere (because ψ' is finite). This **discontinuity condition** (T3.3) will be employed in the treatment of the δ-function well (in section 3.3).

3.1.c Curvature properties. Zeros [B&J p 103-114]

By writing the energy eigenvalue equation on the form

$$\frac{\psi''}{\psi} = -\frac{2m}{\hbar^2}\left[E - V(x)\right], \qquad \text{(T3.4)}$$

we see that this differential equation determines the local *relative curvature* of the wave function, ψ''/ψ, which is seen to be proportional to $E - V(x)$, the kinetic energy.

(i) In **classically allowed regions**, which by definition is where $E > V(x)$, this relative curvature is negative: Then ψ'' is negative wherever ψ is positive, and vice versa. This means that $\psi(x)$ curves towards the x axis:

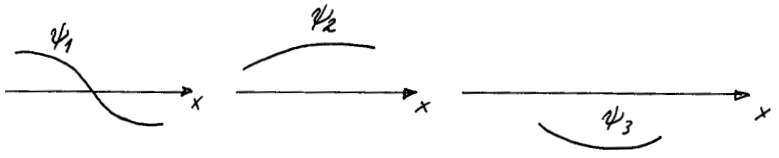

A well-known example is presented by the solutions $\psi_n(x) = \sqrt{2/L}\,\sin k_n x$ for the one-dimensional box. Here,

$$\frac{\psi_n''}{\psi_n} = -\frac{2m}{\hbar^2}\, E_n \equiv -k_n^2, \qquad k_n = n\,\frac{\pi}{L}.$$

Thus a relative curvature which is constant and negetive corresponds to a sinusoidal solution. (See the figure in page 3 of Tillegg 2.) We note that the higher the kinetic energy (E) and hence the wave number (k) are, the faster ψ will curve, and the more zeros we get.

(ii) In **classically forbidden regions**, where $E - V(x)$ is negative, the relative curvature is positive: In such a region, ψ' is positive wherever ψ is positive, etc. The wave function ψ will then curve away from the axis.

A central example is the harmonic oscillator. For a given energy E_n, the particle will according to *classical mechanics* oscillate between two points which are called the **classical turning points**. These are the points where $E_n = V(x)$, that is, where the "energy line" crosses the potential curve. Classically, the regions outside the turning points are forbidden. In quantum mechanics, we call these regions classically forbidden regions. In these regions we note that the energy eigenfunctions $\psi_n(x)$ curve away from the axis.

In the classically *allowed* regions (between the turning points) we see that the energy eigenfunctions $\psi_n(x)$ curve towards the axis (much the same way as the box solutions), and faster the higher E_n (and hence $E_n - V(x)$) are. As for the box, we see that the number of zeros increases for increasing E_n. Then perhaps it does not come as a surprise that

the ground state of a one-dimensional potential does not have any zeros.

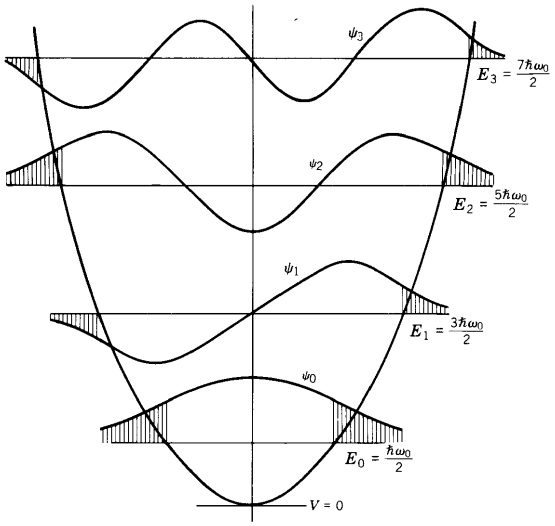

Because $E_n - V(x)$ here depends on x, the eigenfunctions $\psi_n(x)$ are not sinusoidal in the allowed regions. We note, however, that they in general get an oscillatory behaviour. For large quantum numbers (high energies E_n), the kinetic energy $E_n - V(x)$ will be approximately constant locally (let us say over a region covering at least a few "wavelengths"). Then ψ_n will be *approximately* sinusoidal in such a region. An indirect illustration of this is

found on page 58 in Hemmer and in 4.7 in B&J, which shows *the square* of ψ_n, for $n = 20$. (When ψ_n is approximately sinusoidal locally, also $|\psi_n|^2$ becomes sinusoidal; cf the relation $\sin^2 kx = \frac{1}{2}(1 - \cos 2kx)$.) [1]

(iii) In a classical turning point, where $V(x) = E$, we see from (T3.4) that $\psi''/\psi = 0$. This means that the wave function has a turning point in the mathematical sense, where the curvature changes sign. [2]

For *piecewise constant* potentials (see below) it may happen that an energy eigenvalue is equal to one of the constant potential values. We then have $V(x) = E$ i a certain region, so that ψ'' is equal to zero. In this region, ψ itself must then be a linear function, $\psi = Ax + B$. The figure shows a box potential with an extra well in the middle. The size of this well can be chosen in such a way that the energy of the ground state becomes exactly equal to zero. Outside the central well we then have $E = V = 0$, giving a linear wave function in these regions, while it is sinusoidal in the central region.

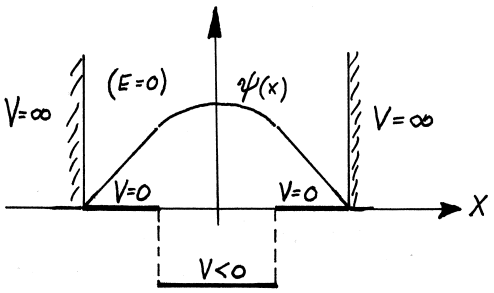

3.1.d Degree of deneracy [B&J p 110]

The one-dimensional box and the one-dimensional harmonic oscillator have **non-degenerate energy levels**. With this we mean that there is only one energy eigenfunction for each energy eigenvalue E_n. It can be shown that this holds for all one-dimensional potentials, for bound states:

> Bound energy levels in one-dimensional potentials are **non-degenerate**, meaning that for each (discrete) energy level there is only one energy eigenfunction. (T3.5)

Since the one-dimensional time-independent Schrödinger equation is of second order, the number of independent eigenfunctions for any energy E is maximally equal to two, so that the **(degree of) deneracy** never exceeds 2. [3] For *unbound states*, we can have degeneracy

[1] When $E - V(x)$ is approximately constant over a region covering one or several wavelengths, we can consider $k(x) \equiv \hbar^{-1}\sqrt{2m(E - V(x))}$ as an approximate "wave number" for the approximately sinusoidal wave function. This "wave number" increases with $E - V(x)$. This is illustrated in the diagrams just mentioned, where we observe that the "wavelength" ($\lambda(x) \equiv 2\pi/k(x)$) is smallest close to the origin, where the kinetic energy is maximal.

[2] For finite potentials we see from (T3.4) that ψ'' is also equal to zero at all the nodes of $\psi(x)$. Thus, all the nodes (zeros) of $\psi(x)$ are mathematical turning points, but at these nodes the *relative* curvature does not change sign; cf the figure above.

[3] **The (degree of) degeneracy** for a given energy level E is defined as the number of linearly independent energy eigenfunctions for this energy.

2, but it also happens that there is only one unbound state for a given energy (see the example below).

Proof (not compulsory in FY1006/TFY4215): These statements can be proved by an elegant mathematical argument: *Suppose* that $\psi_1(x)$ and $\psi_2(x)$ are two energy eigenfunctions with the same energy E. We shall now examine whether these can be linearly independent. From the time-independent Schrödinger equation, on the form

$$\frac{d^2\psi/dx^2}{\psi} \equiv \frac{\psi''}{\psi} = \frac{2m}{\hbar^2}\left[V(x) - E\right], \tag{T3.6}$$

it follows that

$$\frac{\psi_1''}{\psi_1} = \frac{\psi_2''}{\psi_2}, \qquad \text{i.e.,} \qquad \psi_1''\psi_2 - \psi_2''\psi_1 = 0, \tag{T3.7}$$

or

$$\frac{d}{dx}\left(\psi_1'\psi_2 - \psi_2'\psi_1\right) = 0, \quad \text{i.e.,} \quad \psi_1'\psi_2 - \psi_2'\psi_1 = \text{constant, (independent of } x\text{).} \tag{T3.8}$$

If we can find at least one point where both ψ_1 and ψ_2 are equal to zero, it follows that this constant must be equal to zero, and then the expression $\psi_1'\psi_2 - \psi_2'\psi_1$ must be equal to zero for all x. Thus we have that

$$\frac{\psi_1'}{\psi_1} = \frac{\psi_2'}{\psi_2}.$$

This equation can be integrated, giving

$$\ln\psi_1 = \ln\psi_2 + \ln C, \qquad \text{or} \qquad \psi_1 = C\psi_2. \tag{T3.9}$$

Thus, the two solutions $\psi_1(x)$ and $\psi_2(x)$ are *not* linearly independent, but are one and the same solution, apart from the constant C. Thus, if we can find at least one point where the energy eigenfunction must vanish, then there exists only one energy eigenfunction for the energy in question.

This is what happens e.g. for bound states in one dimension. A bound-state eigenfunction must be square-integrable (i.e., localized in a certain sense), so that the wave function approaches zero in the limits $x \to \pm\infty$. Then the above constant is equal to zero, and we have no degeneracy, as stated in (T3.5).

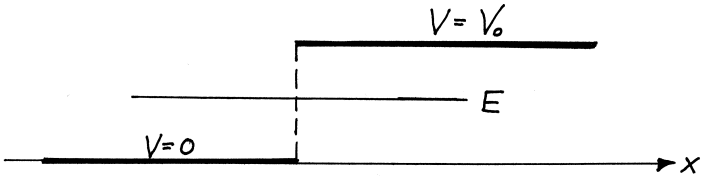

An example is given by the step potential above, for states with $0 < E < V_0$. Here, the solution in the region to the right must approach zero exponentially, because E is smaller than V_0. We can then show that there is only one energy eigenfunction for each energy in the interval $0 < E < V_0$, even if this part of the energy spectrum is continuous. Note that these states are unbound, because the eigenfunctions are sinusoidal in the region to the left.

For $E > V_0$, on the other hand, it turns out that we have two solutions for each energy, as is also the case for the free particle in one dimensjon.

Some small exercises:

1.1 Show that the classically allowed region for the electron in the ground state of the hydrogen atom is given by $0 \leq r < 2a_0$, where a_0 is the Bohr radius.

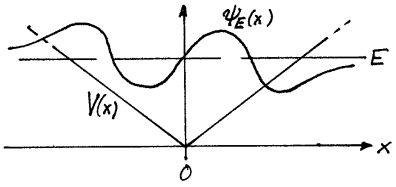

1.2 The figure shows a potential $V(x) = k|x|$ and a sketch of an energy eigenfunction $\psi_E(x)$ with energy E for this potential.
a. Why is E the third excited energy level for this potential?
b. Show that the classical turning points for the energy E lie at $x = \pm E/k$.
c. Why must possible zeros of an energy eigenfunction for this potential lie between the classical turning points for the energy in question? [Hint: Consider the curvature outside the classical turning points.]
d. Why has this potential no unbound energy eigenstates?

3.1.e Symmetric potentials [Hemmer p 71, B&J p 159]

For **symmetric potentials**, we shall see in chapter 4 that it is possible to find energy eigenfunctions (eigenfunctions of $\widehat{H}$) which are either symmetric or antisymmetric.

For *bound* states, corresponding to non-degenerate energy levels, it turns out that the energy eigenfunctions for a symmetric potential *have to* be either symmetric or antisymmetric. Well-known examples are the box eigenstates (with $x = 0$ at the midpoint of the box) and the eigenfunctions of the harmonic oscillator, which are alternating symmetric and antisymmetric. The same holds for the bound states of the (finite) square well. For the latter case, we shall see that the symmetry properties simplify the calculations.

In cases where there are *two* energy eigenfunctions for each energy (which happens for *unbound* states), *it is possible* to find energy eigenfunctions with definite symmetry (that is, one symmetric and one antisymmetric solution), but in many cases it is then relevant to work with energy eigenfunctions which are **asymmetric** (linear combinations of the symmetric and the antisymmetric solution). This is the case e.g. in the treatment of scattering against a potential barrier and a potential well (see section 3.6 below).

3.2 The square well [Hemmer 3.3, B&J 4.6]

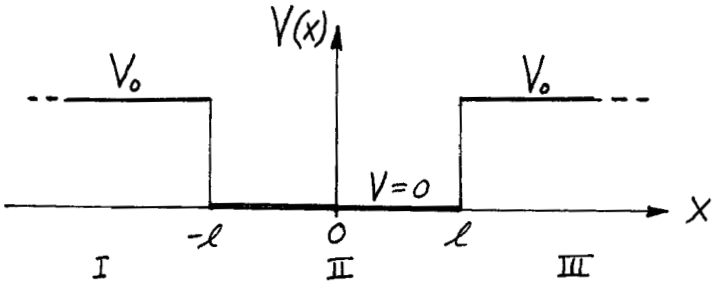

The finite potential well, or **square well**, is useful when we want to *model* so-called **quantum wells** or **hetero structures**. These are semiconductors consisting of several layers of different materials. In the simplest case, the region between $x = -l$ and $x = +l$ represents a layer where the electron experiences a lower potential energy than outside this layer. When we disregard the motion *along* the layer (in the y and z directions), this can be described (approximately) as a one-dimensional square well.

3.2.a General strategy for piecewise constant potentials

The potential above is an example of a so-called **piecewise constant potential**. The strategy for finding energy eigenfunctions for such potentials is as follows:

1. We must consider the *relevant energy regions* separately. (In this case these are $E > V_0$ and $0 < E < V_0$).

2. For a given energy region (e.g. $E < V_0$), we can find the general solution of the time-independent Schrödinger equation $\widehat{H}\psi = E\psi$ for each region in x (here I, II and III), expressed in terms of two undetermined coefficients: [4]

(i) In classically *allowed* regions, where $E - V > 0$, we then have

$$\psi'' = -\frac{2m}{\hbar^2}(E-V)\psi \;\equiv\; -k^2\psi; \qquad k \equiv \frac{1}{\hbar}\sqrt{2m(E-V)}, \tag{T3.10}$$

with the general solution

$$\psi = A\sin kx + B\cos kx. \tag{T3.11}$$

(ii) In classically *forbidden* regions, where $E < V$, we have

$$\psi'' = \frac{2m}{\hbar^2}(V-E)\psi \;\equiv\; \kappa^2\psi\;; \qquad \kappa \equiv \frac{1}{\hbar}\sqrt{2m(V-E)}, \tag{T3.12}$$

with the general solution [5]

$$\psi = Ce^{-\kappa x} + De^{\kappa x}. \tag{T3.13}$$

Try to always remember this:

> Sinusoidal solutions (curving towards the x axis) in classically allowed regions; exponential solutions (curving outwards) in classically forbidden regions. (T3.14)

3. The last point of the program is: *Join together* the solutions for the different regions of x in such a way that both ψ and $\psi' = d\psi/dx$ become continuous (smooth joint). Possible boundary condtions must also be taken into account, so that resulting solution $\psi(x)$ becomes

[4] Remember that the second-order differential equation $\widehat{H}\psi = E\psi$ always has two independent solutions, locally.

[5] (iii) In exceptional cases, when $E = V$ in a finite region, we have $\psi'' = 0$, so that the general solution in this region is $\psi = Ax + B$.

an acceptable eigenfunction of $\widehat{H}$. (This programme must be implemented for each of the relevant energy regions mentioned under 2 above.)

NB! When ψ and ψ' both are continuous, we note that also ψ'/ψ is continuous. It is often practical to use the continuity of ψ together with that of ψ'/ψ, as we shall soon see. (The quantity ψ'/ψ is called the logarithmic derivative, because it is the derivative of $\ln\psi$.)

3.2.b Bound and unbound states

For $E > V_0$ one finds that the energy spectrum of the square well is continuous, with two independent energy eigenfunctions for each energy, as is the case for a free particle. These wave functions describe *unbound* states, which are not square integrable.

For $E < V_0$ one finds that the energy is quantized, with one energy eigenfunction for each of the discrete energy levels. These levels thus are non-degenerate. This is actually the case for all bound states in one-dimensional potentials.

> As discussed above, it turns out that the bound-state energy eigenfunctions are alternating symmetric and antisymmetric with respect to the midpoint of the symmetric well: The ground state is symmetric, along with the second excited state, the 4th, the 6th, etc. The first excited state is antisymmetric, along with the third excited state, the 5th, the 7th, etc. These properties actually are the same for all bound states in symmetric one-dimensional potentials. (See Tillegg 4, where this property is proved.)

The "moral" is that when we want to find bound states in a symmetric potential, we can confine ourselves to look for energy eigenfunctions that are either symmetric or antisymmetric.[6]

3.2.c Boundary conditions and continuity leads to energy quantization

As in B&J, we shall now see how the energy eigenvalues and the energy eigenfunctions can be obtained, assuming that the eigenfunctions are either symmetric or antisymmetric. Following the general procedure outlined above, we write down the general solutions for each of the regions I, II and III:

I: $x < -l$	II: $-l < x < l$	III: $x > l$
$\psi = Ce^{\kappa x} + De^{-\kappa x}$	$\psi_S = B\cos kx$ $\psi_A = A\sin kx$	$\psi = C'e^{-\kappa x} + D'e^{\kappa x}$
$\kappa = \frac{1}{\hbar}\sqrt{2m(V_0 - E)}$	$k = \frac{1}{\hbar}\sqrt{2mE}$	
$\psi'/\psi = \kappa$	$\psi'_S/\psi_S = -k\tan kx$ $\psi'_A/\psi_A = k\cot kx.$	$\psi'/\psi = -\kappa$

[6] Hemmer shows how these symmetry properties emerge when one solves the eigenvalue equation (explicitly), without assuming symmetry or antisymmetry. Thus these properties are determined by the eigenvalue equation. In section 3.3 we shall see how this works for the harmonic oscillator potential.

Here, there are several points worth noticing:

(i) Firstly, we must take into account the following **boundary condition**: An eigenfunction is not allowed to diverge (become infinite), the way $D'\exp(\kappa x)$ does when $x \to \infty$ or the way $D\exp(-\kappa x)$ does when $x \to -\infty$. Therefore we have to set the coefficients D and D' equal to zero.

(ii) Secondly, the general solution for region II (inside the well) really is $\psi = A\sin kx + B\cos kx$. However, here we can allow ourselves to assume that the solution is either symmetric ($\psi_S = B\cos kx$, and $C' = C$) or antisymmetric ($\psi_A = A\sin kx$ and $C' = -C$).

(iii) But still we have not reached our goal, which is to determine the energy. The figure shows how the "solution" would look for an *arbitrary* choice of E.

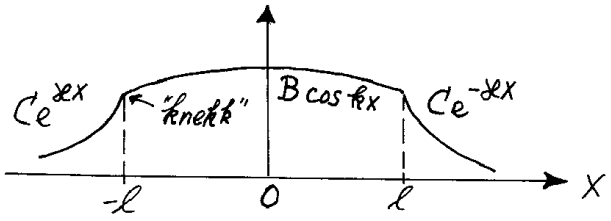

Here we have chosen B/C such that ψ is continuous for $x = \pm l$. But as we see, the resulting function $\psi(x)$ has "kinks" for $x = \pm l$; the joints are not *smooth*, as they should be for an eigenfunction.

We could of course make the kinks go away by adding a suitable bit of the solution $De^{\kappa x}$ to the solution for region III, on the right (and similarly on the left). But then the resulting solution would diverge in the limits $x \to \pm\infty$, and that is not allowed for an eigenfunction, as stated above.

The "moral" is that there is no energy eigenfunction for the energy chosen above. If we try with a slightly higher energy E (corresponding to a slightly larger wave number k in region II), the cosine in region II will curve a little bit *faster* towards the x axis, while $C\exp(\pm\kappa x)$ on the right and on the left will curve a little bit slower (because $\kappa \propto \sqrt{V_0 - E}$ becomes smaller when E increases). If we increase E *too* much, the cosine will curve too much, so that we get kinks pointing the other way. Thus, it is all a matter of finding the particular value of the energy for which there is no kink.

As you now probably understand, we get energy quantization for $0 < E < V_0$; only one or a limited number of energies will give smooth solutions, that is, energy eigenfunctions. The correct values of E are found in a simple way by using the continuity of the logartithmic derivative ψ'/ψ for $x = -l$. This leads to the conditions

$$\kappa = \begin{cases} k\tan kl & (S), \\ -k\cot kl = k\tan(kl - \frac{1}{2}\pi) & (A), \end{cases} \tag{T3.15}$$

for respectively the symmetric and the antisymmetric case. Multiplying by l on both sides and using the relations

$$kl = \frac{l}{\hbar}\sqrt{2mE} \qquad \text{and} \qquad \kappa l = \frac{l}{\hbar}\sqrt{2m(V_0 - E)} = \sqrt{\frac{2mV_0l^2}{\hbar^2} - (kl)^2},$$

we can write the conditions on the form

$$\kappa l = \sqrt{\frac{2mV_0l^2}{\hbar^2} - (kl)^2} \;\; = \;\; kl\tan kl \qquad (S),$$

(T3.16)

$$\kappa l = \sqrt{\frac{2mV_0l^2}{\hbar^2} - (kl)^2} \;\; = \;\; kl\tan(kl - \tfrac{1}{2}\pi) \qquad (A),$$

where both the left and right sides are functions of kl, that is, of the energy E. Since the left and right sides are *different* functions of kl, we understand that these conditions will be satisfied only for certain discrete values of kl. The k values can be determined graphically by finding the ponts of intersection between the tangent curves (right side) and the left side. As a function of kl we see that the left side is a quarter of a circle with radius

$$\sqrt{\frac{2mV_0l^2}{\hbar^2}} \equiv \gamma. \tag{T3.17}$$

This radius (which is here denoted by γ) depends on the *parameters* in this problem, which are the mass m and the parameters V_0 and l of the well.

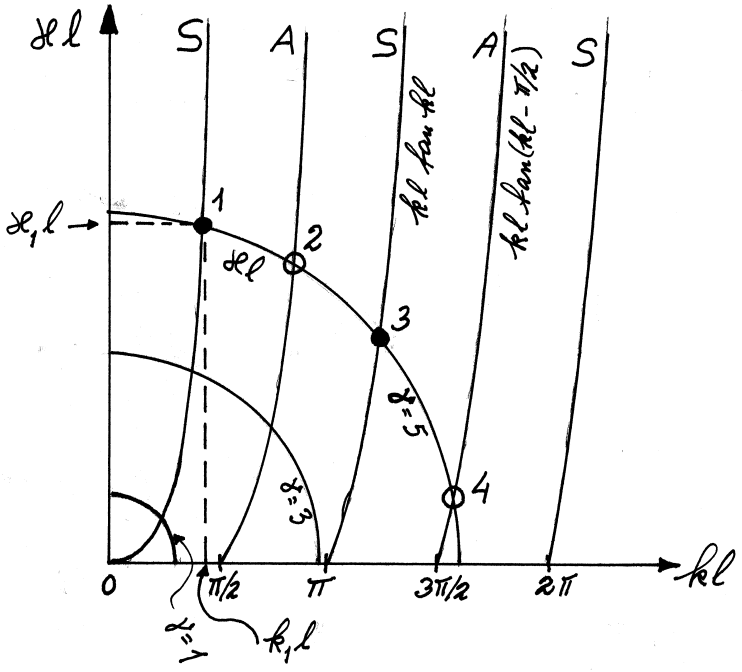

The figure shows the tangent curves, which are independent of the parameters, and the points of intersection between these curves and the circle κl for a radius $\gamma = 5$. In this case we find two symmetric solutions (see the filled points 1 and 3) and two antisymmetric solutions (see the "open" points 2 and 4).

By reading out the coordinates k_il and κ_il of these points of intersection, we can find the energies and the binding energies of the ground state (1) and the three excited states (2,3,4) which are found for a well with $\gamma = 5$. These are respectively [7]

$$E_i = \frac{\hbar^2k_i^2}{2m} = \frac{\hbar^2(k_il)^2}{2ml^2}\,; \qquad (E_B)_i \equiv V_0 - E_i = \frac{\hbar^2\kappa^2}{2m} = \frac{\hbar^2(\kappa_il)^2}{2ml^2}, \quad i = 1, 4. \tag{T3.18}$$

[7] The binding energy is defined as the energy that must be supplied to liberate the particle from the well, here $V_0 - E$.

3.2.d Discussion

From the figure above it is clear that the *number* of bound states depends on the dimensionless quantity $\gamma = \sqrt{2mV_0l^2/\hbar^2}$, that is, on the mass and the parameters V_0 and l of the well. For $\gamma = 3$, we see that there are only two bound states. The diagram also tells us that if γ does not exceed $\pi/2$, there is only one bound state. For $\gamma < \pi/2$ (e.g. $\gamma = 1$) we thus have only one bound state, the symmetric ground state. The bound ground state, on the other hand, exists no matter how small γ is, that is, no matter how narrow and/or shallow the well is.

Let us now imagine that the product V_0l^2 is gradually increased, corresponding to a gradual increase of γ. From the diagram we then understand that a new point of intersection will appear every time γ passes a multiple of $\pi/2$. This simply means that the number of bound states equals 1 + the integer portion of $\gamma/(\frac{1}{2}\pi)$:

$$\text{number of bound states} = 1 + \left[\frac{1}{\frac{1}{2}\pi}\sqrt{2mV_0l^2/\hbar^2}\right] \tag{T3.19}$$

(where $[z]$ stands for the largest integer which is smaller than z. For example, $[1.7] = 1$).

From the figure we also see that when γ has just passed a multiple of $\pi/2$, then the value of κl for the "newly arrived" state is close to zero. The same then holds for the binding energy $E_B = \hbar^2(\kappa l)^2/(2ml^2)$. The "moral" is that when the well (that is, γ) is just large enough to accomodate the "new" state, then this last state is very **weakly bound**. This also means that the wave function decreases very slowly in the classically forbidden regions. [For example, $C\exp(-\kappa x)$ decreases very slowly for $x > l$ when κ is close to zero.]

The figure on the left below gives a qualitative picture of the resulting (bound-state) eigenfunctions of a well which is large enough to accomodate three bound states.

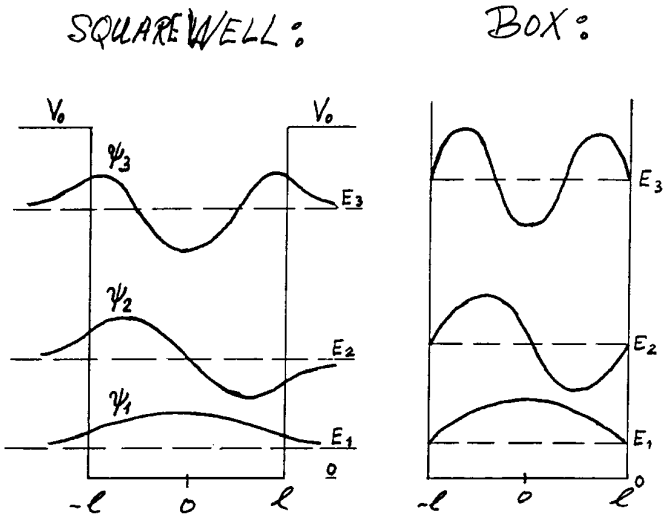

For comparison, the figure on the right shows the first three solutions for a box of the same width ($2l$) as the well. In both cases we have used the "energy lines" as "x axis" (abscissa axis). There is a lot of "moral" to be gained from these graphs:

(i) The box may be viewed as a well in the limit where V_0 goes to infinity. We see that for the well, with a finite V_0, the eigenfunctions $\psi_n(x)$ "penetrate" into the classically forbidden regions (where $E < V_0$). On the right side, this penetration takes place in terms of the

"exponential tail" $C\exp(-\kappa x)$. This kind of penetration into classically forbidden regions is characteristic for all bound states; the wave functions — and hence also the probability densities — are different from zero in regions where the particle can not be found according to classical mechanics.

In the case at hand, we see that the probability density at the position $x = l + \frac{1}{2\kappa}$ is reduced by a factor $1/e$ compared to the value at $x = l$. Therefore, we may *define* the length $1/2\kappa$ as a **penetration depth**:

$$l_{\text{p.d.}} \equiv \frac{1}{2\kappa} = \frac{\hbar}{\sqrt{2m(V_0 - E)}} \qquad \text{(penetration depth).} \tag{T3.20}$$

We see that this penetration depth decreases for increasing $V_0 - E$. The larger $V_0 - E$ is, the "more forbidden" is the region on the right, and the smaller the penetration depth becomes.

(ii) We also notice that the penetration makes the wavelengths λ_i in the classically *allowed* regions smaller than the corresponding wavelengths for the box. The wave *numbers* $k_i = 2\pi/\lambda_i$ then become a little smaller than for the box, and the same holds for the energies, as is indicated in the figure above.[8]

(iii) Apart from these differences, we observe that the box model gives a *qualitatively* correct picture of the well solutions. For a larger well, with a larger number of bound states, these differences become less important. We should also keep in mind that even the square well is only an idealized model of a more realistic well potential (which is continuous, unlike the square well). For such a realistic well, the mathematics will be even more complicated than for the square well.

Based on the comparison above, we expect that a square well will give a reasonably correct description of the states of a more realistic well, and many of the properties of the square-well solutions are fairly well described by the box model. In all its simplicity the box model therefore is a much more important model in quantum mechanics than one might believe from the start.

Important examples are as mentioned heterostructures used in electronics, optics and optoelectronics. The width then typically is several nanometers, which means that we have to do with fairly wide wells, with a large number of states. The box approximation may then be quite good.

Another example from solid-state physics is the **free-electron-gas model**, where a piece of a metal can be considered as a potential well, in which a large number of conduction electrons (one or more per atom) are moving approximately as free particles in the metal volume. For such a well of macroscopic dimensions, the box model is an excellent approximation.

[8] The same message is obtained from the figure on page 11. Here the abscissa of the point of intersection is $k_j l$, and in the figure you can observe that $k_j l$ is always smaller than j times $\pi/2$. Note that the corresponding wave number for box state number j is given by

$$k_j^{\text{box}} \cdot 2l = j \cdot \pi, \quad \text{that is,} \quad k_j^{\text{box}} l = j\pi/2.$$

Some small exercises:

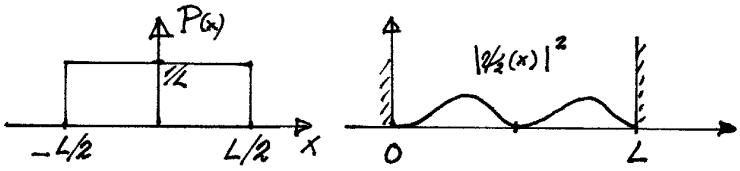

2.1 The figure on the left shows a probability density $P(x)$ distributed evenly over the interval $(-\frac{1}{2}L, \frac{1}{2}L)$.
a. Argue that the root of the mean square deviation from the mean value (Δx) is larger than $\frac{1}{4}L$.
b. *Show* that $\Delta x = L/\sqrt{12} \approx 0.29\,L$.
c. The graph on the right shows the probability density $|\psi_2(x)|^2$ of the energy state ψ_2 for a particle in a box. What is the expectation value $\langle\, x \,\rangle$ here? Argue that Δx is larger than $\frac{1}{4}L$.

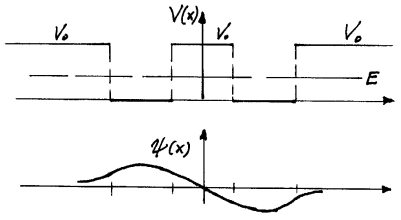

2.2 The figure above shows a potential $V(x)$ and a funktion $\psi(x)$. Why cannot this fuction $\psi(x)$ be an energy eigenfunction for the energy E marked in the figure? [Hint: What is wrong with the curvature?]

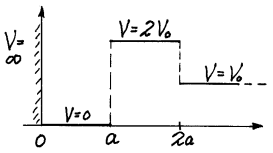

2.3 Why has the potential in the figure no bound states (energy eigenfunctions) with energy $E > V_0$? [Hint: Check the general solution of the time-independent Schrödinger equation for $x > 2a$ and $E > V_0$.]

2.4 Use the diagram on page 11 to answer the following questions:
a. Even for a very small well ($\gamma = \sqrt{2mV_0l^2/\hbar^2} \to 0$) there is always one bound state. Check that $E \to V_0$ and $E_B/E \to E_B/V_0 \to 0$ when $\gamma \to 0$. [Hint: E_B/E can be expressed in terms of the ratio κ/k.]
b. If we let the "strength" γ of the well increase gradually, the first excited state will appear just when γ passes $\frac{1}{2}\pi$. What can you say about E and E_B/E for this state when γ is only slightly larger than $\frac{1}{2}\pi$? What can you say about E and E_B/E for the second excited state when γ is only slightly larger than π?

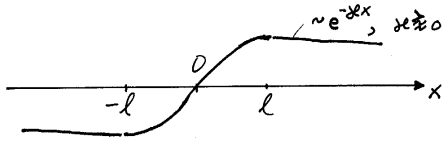

2.5 The figure shows an energy eigenfunction for the well, which behaves as $\psi \sim e^{-\kappa x}$ for $x > l$, where κ is positive, but very close to zero. How large is the binding energy $E_B = V_0 - E$ of this state? How large is the wave number k (for the solution in the classically allowed region)? How large is the "strength" γ of the well?

2.6 Show that the penetration depth for an electron with $E_B = V_0 - E = 1$ eV is approximately 2 Ångstrøm.

3.2.e Discussion of energy quantization based on curvature properties***[9]

It is instructive to study the energy quantization in light of the curvature properties of the eigenfunctions. As discussed on page 3, the eigenvalue equation determines the relative curvature

$$\frac{\psi''}{\psi} = -\frac{2m}{\hbar^2}\left[E - V(x)\right] \tag{T3.21}$$

of the eigenfunction, as a function of $V(x)$ and E.

Let us imagine that we use a computer program to find a numerical solution of this equation for a given potential $V(x)$, and for a chosen energy value E, which we *hope* will give us an energy eigenfunction.

If we specify the value of ψ and its derivative ψ' in a starting point x_0, the computer can calculate $\psi''(x_0)$ [using $\psi(x_0)$, E and $V(x_0)$]. From $\psi(x_0)$, $\psi'(x_0)$ and $\psi''(x_0)$, it can then calculate the values of ψ and ψ' at a neighbouring point $x_0 + \Delta x$. The error in this calculation can (with an ideal computer) be made arbitrarily small if we choose a sufficiently small increment Δx. By repeating this process the computer can find a numerical solution of the differential equation. In the following discussion we shall assume an ideal computer, which works with a negligible numerical uncertainty.

Example: Particle in box ($V = 0$ for $-l < x < l$, infinite outside)

We know that the *eigenfunctions* of the box are either symmetric or antisymmetric. (See page 7.)

(i) The computer will return a **symmetric solution** if we choose the origin as the starting point and specify that $\psi'(0) = 0$ (ψ flat at the midpoint) and $\psi(0) = 1$ (arbitrary normalization). In addition, we must give the computer an energy E. If we give it one of of the energy eigenvalues

$$E_n = E_1 n^2, \qquad n = 1, 3, 5, \cdots, \qquad E_1 = \frac{\hbar^2 k_1^2}{2m}, \qquad k_1 \cdot 2l = \pi, \tag{T3.22}$$

[9] Not compulsory.

obtained in section 2.1 for symmetric eigenfunctions, the computer will reproduce the corresponding eigenfunction. Thus, if we choose e.g. the ground-state energy E_1, the computer will reproduce the cosine solution $\psi_{E_1} = \cos(\pi x/2l)$, which curves just fast enough to approach zero at the boundaries, $x = \pm l$; cf the figure. [10]

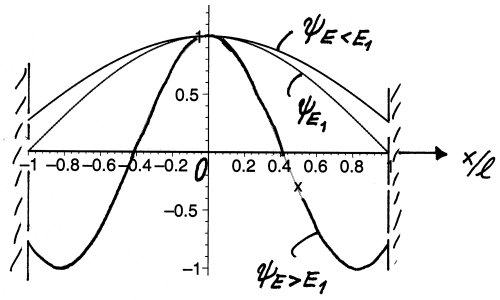

It is also interesting to examine what happens if we ask the computer to try with an energy E which is *lower* than the ground-state energy E_1, with the same starting values as above. The computer will then return a "solution" $\psi_{E<E_1}$ which curves too slowly, so that it still has a positive value $\psi_{E<E_1}(l) > 0$ at the boundary $x = l$, and thus does not satisfy the boundary condition (continuity at $x = \pm l$), as shown in the figure. Thus the computer finds a "solution" for each E smaller than E_1, but this "solution" is not an energy eigenfunction.

In the figure above we have also included a solution $\psi_{E>E_1}$. This solution curves faster than the ground state (because $E > E_1$), but not fast enough to satisfy the boundary condition, as we see. By sketching some solutions of this kind, you will realize that none of the symmetric "solutions" for $E_1 < E < E_3$ will satisfy the boundary conditions. This illustrates the connection between the curvature properties of the "solutions" and energy quantization.

(ii) In a similar manner, we can examine **antisymmetric** solutions, by giving the computer the starting values $\psi(0) = 0$ and $\psi'(0) = 1$. If we then try with the energy $E = E_2$ of the first excited state, the computer will retuen the energy eigenfunction $\psi_{E_2}(x)$, as shown in the figure below. If we try with E *less than* E_2, the curvature of the "solution" $\psi_{E<E_2}(x)$ becomes too small to give an eigenfunction (see the figure).

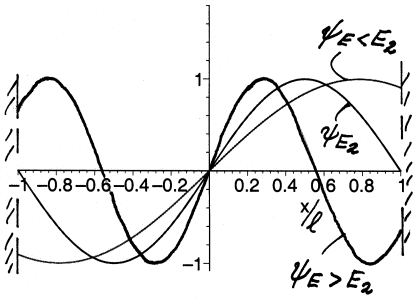

We note that the reason that the first excited state ψ_{E_2} has a higher curvature than the ground state is that is has a zero, as opposed to the ground state. (We are not counting the zeros on the boundary.)

(iii) An alternative to the procedures (i) and (ii) above is to start at the boundary on the left, with the values $\psi(-l) = 0$ and $\psi'(-l) \neq 0$. The diagram below shows two "solutions", one with $E < E_1$, and one with $E_1 < E < E_2$.

[10] Note that with the origin at the midpoint, all the symmetric solutions go as cosine sulutions, while the symmetric ones go as sines.

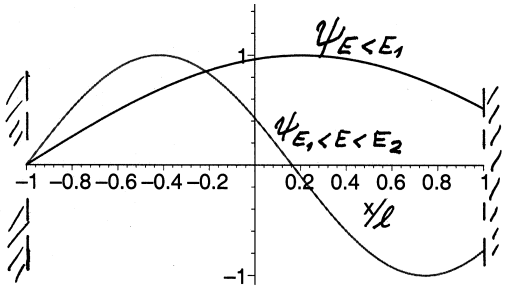

Again we see that the curvature and hence the number of zeros increase with the energy. All these solutions with a zero at $x = -l$ are of the type $\psi = \sin[k(x + l)]$, where $k = \sqrt{2mE/\hbar^2}$. An energy eigenfunction is obtained every time ψ equals zero on the boundary on the right, that is, for $k_n \cdot 2l = n\pi$. The eigenfunctions $\psi_n = \sin[k_n(x + l)]$ are of course exactly the same as found before.

Square well

Similar numerical "experiments" can be made for the square well. We can let the computer look for energy eigenfunctions by asking it to try for all energies in the interval $0 < E < V_0$.

The figure below illustrates what happens if we ask the computer to try with an energy which is lower than the ground-state energy E_1. Starting with $\psi'(0) = 0$ and $\psi(0) = 1$ for a symmetric solution (as under (i) above), the computer will than return a solution which curves slower than than the ground state ψ_{E_1} in the classically allowed region, as shown in the figure. This "solution" therefore becomes less steep than the ground state at the points $x = \pm l$.

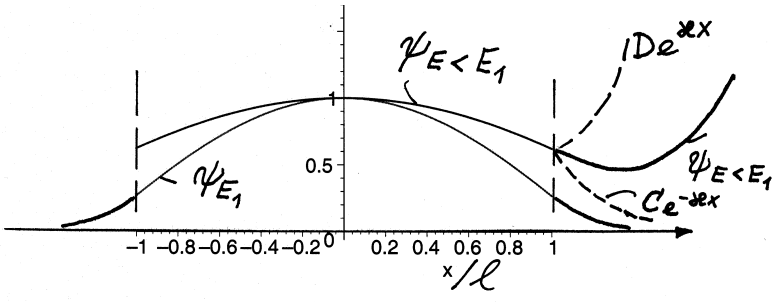

Outside the well, the relative curvature *outwards* from the axis will be faster than for the ground state (because $\kappa = \sqrt{2m(V_0 - E)/\hbar^2}$ is larger than κ_1). This "solution" therefore cannot possibly approach the x axis smoothly (the way the ground state ψ_{E_1} does); it "takes off" towards infinity, as illustrated in the figure. [11] For $x > l$, the "solution" is now a linear combination of the acceptable function $C\exp(-\kappa x)$ and the unacceptable function $D\exp(\kappa x)$. It will therefore approach infinity when x goes towards infinity. [12]

[11] Note that the computer does not create any "kink" in the "solution" ψ. Because $\psi'' = (2m/\hbar^2)[V(x) - E]\psi$ is finite, ψ' and ψ become continuous and smooth at the points $x = \pm l$.

[12] From such a figure, we can also understand why there always exists a *bound* ground state, no matter how small the well is, as mentioned on page 12. For a tiny well, the cosine solution in the allowed region only develops a very small slope, so that ψ is almost "flat" at $x = \pm l$. But no matter how flat this cosine is, we can always find an energy slightly below zero such that $\kappa = \sqrt{2m(V_0 - E)/\hbar^2}$ becomes small enough to make $C\exp(-\kappa x)$ just as flat at $x = l$, giving a smooth joint. In such a case, the binding

An alternative, as in (iii) above, is to start with a "solution" $\psi_{E<E_1}$ going as (the acceptable function) $C\exp(\kappa x)$ for $x < -l$. In the figure, we have chosen to give this solution the value 1 at $x = -l$, and the same has been done for the ground state ψ_{E_1}, which is also shown in the diagram. At the point $x = -l$ the slopes of the two curves then are

$$\psi'_{E<E_1}(-l) = \kappa = \sqrt{2m(V_0 - E)/\hbar^2} \qquad \text{and} \qquad \psi'_{E_1}(-l) = \kappa_1 = \sqrt{2m(V_0 - E_1)/\hbar^2},$$

and we note that with $E < E_1$ we have $\kappa > \kappa_1$. When the computer works its way through the allowed region, from $x = -l$ to $x = l$, we then note that $\psi_{E<E_1}$ starts out with a *steeper* slope than the ground state ψ_{E_1}. In addition, it curves slower towards the axis than ψ_{E_1} in the entire allowed region. Therefore it arrives at $x = l$ with a larger value and a smaller slope than the ground state. For $x > l$, this solution curves faster outwards than ψ_{E_1}. These are the reasons that this "solution" $\psi_{E<E_1}$ does not "land" on the x axis at all, but increases towards infinity, as illustrated in the figure.

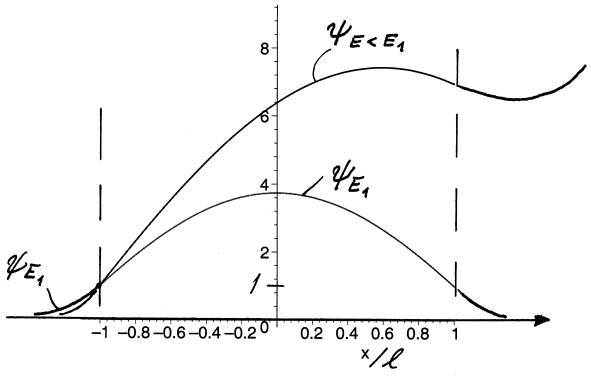

To find an eigenfunction in addition to the ground state, we can repeat the above procedure, but now with $E > E_1$, which gives a faster curvature in the allowed region. The first eigenfunction which then appears is the one with one zero, at $x = 0$. This is the antisymmetric first excited state.

3.2.f More complicated potentials

Based on the curvature arguments above we can now understand why the number of zeros of energy eigenstates increases with the energy, not only for the box and the well above, but also for more realistic potentials.

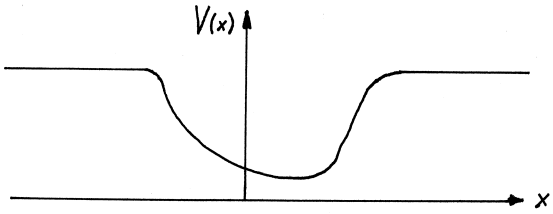

For such an asymmetric potential the energy eigenfunctions will not have a definite symmetry (i.e. be symmetric or antisymmetric as above), but the following properties hold also here:

energy $E_B = \hbar^2\kappa^2/2m$ becomes very small, and the exponential "tail" $C\exp(-\kappa x)$ penetrates far into the forbidden region on the right, and similarly on the left.

- The energies of the bound states are quantized.
- The wave functions of the bound states are *localized*, in the sense that they approach zero quickly at large distances.
- The number of bound states depends on the size of the well.
- The energies of the eigenfunctions increase with the number of zeros (nodes). The ground state has no zero. The first excited state has one zero, and so on.
- For a symmetric potential, the ground state is symmetric, the first excited state is antisymmetric, the second is symmetric, and so on.

A small exercise:
a. Let $\psi(x)$ be a bound energy eigenstate of a square well, or of a harmonic oscillator potential. Why must all the zeros of $\psi(x)$ lie in the classically allowed region? [Hint: Consider the behaviour of $\psi(x)$ in the classically *forbidden* regions.]
b. Does the above rule hold for *all* potentials $V(x)$, that is, must the zeros of an energy eigenfunction $\psi(x)$ always lie in the classically allowed region(s)? [Hint: Consider a symmetric potential for which the origin lies in a classically forbidden region.]

3.3 Delta-function well [Hemmer 3.4]

We shall see that the δ-function potential,

$$V(x) = -\beta\delta(x), \tag{T3.23}$$

is a very simple but also a very special model potential. We may think of it as a square well $V_l(x)$, with a width $2l$ and depth $V_0 = \beta/2l$, in the limit $l \to 0$:

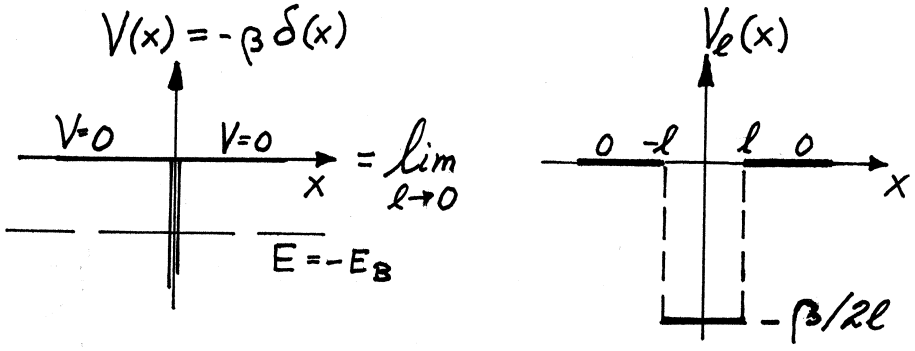

Here we have chosen to set $V = 0$ *outside* the well. We do this because it turns out that the energy of the bound state, $E = -E_B$, approaches a finite value in the limit where the depth of the square well goes to infinity, i. e. in the limit $l \to 0$. (And then of course it doesn't make sense to measure the energy from the bottom of the well, as we are used to do.)

For the model potential on the left, it is very easy to solve the eigenvalue problem. Outside the delta well, where $V = 0$, the eigenvalue equation takes the form

$$\psi'' = \frac{2m}{\hbar^2}[V(x) - E]\psi = \frac{2m}{\hbar^2}[-E]\psi \equiv \kappa^2\psi, \tag{T3.24}$$

with

$$\kappa \equiv \frac{1}{\hbar}\sqrt{2m(-E)} = \frac{1}{\hbar}\sqrt{2mE_B} \qquad \left(E = -\frac{\hbar^2\kappa^2}{2m} = -E_B\right).$$

This equation has the solutions $e^{\kappa x}$ and $e^{-\kappa x}$. Since only the last one is accceptable for $x > 0$ and only the first one for $x < 0$, it follows from the continuity condition that the solution is symmetric:

$$\psi = \begin{cases} Ce^{-\kappa x} & \text{for} \quad x > 0, \\ Ce^{\kappa x} & \text{for} \quad x < 0. \end{cases}$$

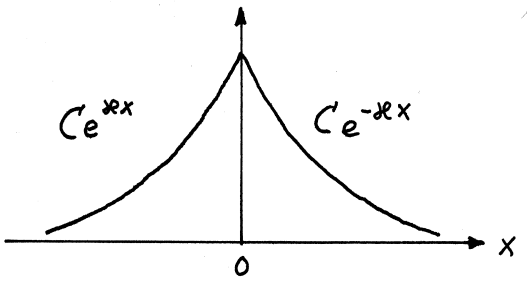

Here, we should not be surprised to find that the function has a cusp, corresponding to a jump in the derivative, at $x = 0$. This is precisely what is required when the potential contains a delta function: According to the discontinuity condition (T3.3), we have (with $\alpha = -\beta$)

$$\psi'(0^+) - \psi'(0^-) = \frac{2m(-\beta)}{\hbar^2}\psi(0). \tag{T3.25}$$

For a given "strength" (β) of the well, this condition determines the quantity κ: The condition (T3.25) gives

$$C(-\kappa) - C(\kappa) = -\frac{2m\beta}{\hbar^2}C, \qquad \text{or} \qquad \kappa = \frac{m\beta}{\hbar^2}.$$

This also determines the energy:

$$E = -\frac{\hbar^2\kappa^2}{2m} = -\frac{m\beta^2}{2\hbar^2}. \tag{T3.26}$$

Thus, the delta-function well is a somewhat peculiar potential model: It has one and only one bound state (with a binding energy which is proportional to the square of the strength parameter β).

We notice that this state is symmetric, as always for a symmetric potential. (You should also note that the eigenvalue equation does not determine the normalization constant. As usual, this is found using the normalization condition, which gives $|C| = \sqrt{\kappa}$.)

Why is there only one bound state? The answer follows when we consider the well with finite width $2l$ and depth $V_0 = \beta/2l$. When this well is made very deep and narrow, i.e. approaches the δ well in the limit $l \to 0$, we see from (T3.25) that the curvature of the cosine in the well region is is large enough to provide the necessary change $\psi_1'(l) - \psi_1'(-l)$ in the derivative (see the figure on the left).

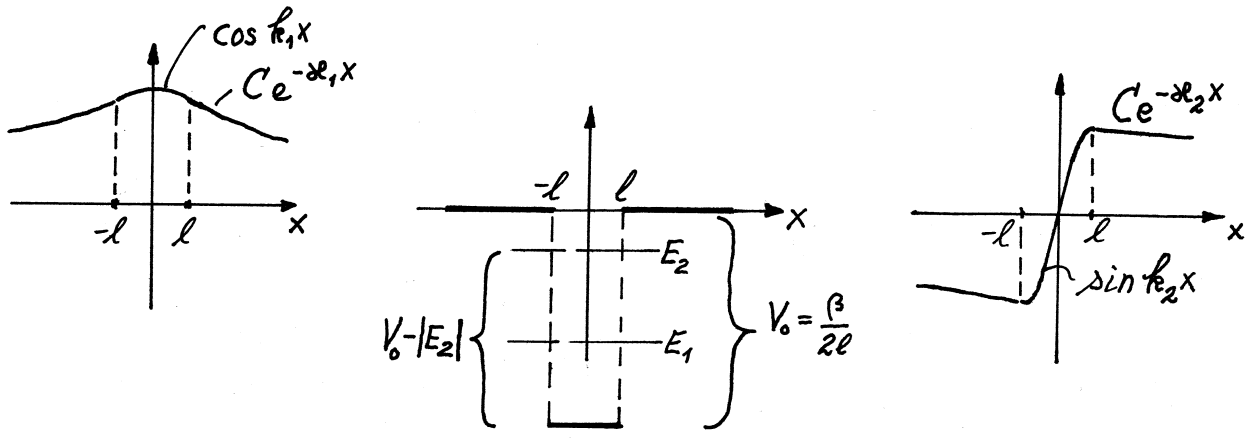

A first excited state ψ_2 (with energy E_2), on the other hand, would require a much larger curvature in the well region. As seen in the figure on the right, the wave number k_2 of the solution $\sin k_2 x$ in the well region must be so large that it allows $\sin k_2 x$ to pass a maximum before $x = l$, so that it can connect smoothly to $Ce^{-\kappa_2 x}$ for $x > l$. This requires that $k_2 l$ is larger than $\pi/2$. However, k_2 is limited by the inequality

$$k_2 = \frac{1}{\hbar}\sqrt{2m(V_0 - |E_2|)} < \frac{1}{\hbar}\sqrt{2mV_0},$$

so that

$$k_2 l < \frac{1}{\hbar}\sqrt{2m\frac{\beta}{2l}l^2} = \frac{1}{\hbar}\sqrt{m\beta l},$$

which approaches zero in the limit $l \to 0$ (instead of being larger than $\pi/2$). As a consequence, only the symmetric ground state survives when l is made sufficiently small, and when it goes to zero, as it does in the delta potential.

3.4 One-dimensional harmonic oscillator

[Hemmer 3.5, Griffiths p 31, B&J p 170]

3.4.a Introduction: The simple harmonisc oscillator

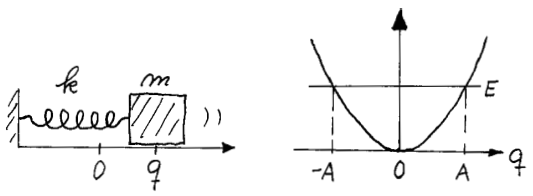

The prototype of a harmonic oscillator is a point mass m attached to the end of a spring with spring constant k, so that the force on the mass is proportional to the displacement (here denoted by q) from the equilibrium position ($q = 0$). With this choice of origin, the force and the potential are

$$F(q) = -kq \qquad \text{and} \qquad V(q) = \tfrac{1}{2}kq^2,$$

if we also choose to set $V(0)$ equal to zero. According to classical mechanics this particle will oscillate (if it isn't at rest). Inserting the trial solution

$$q(t) = A' \cos \omega t + B' \sin \omega t = A \cos(\omega t - \alpha)$$

into Newton's second law, $d^2q/dt^2 = F/m$, we find that the angular frequency of the oscillation is

$$\omega = \sqrt{k/m}.$$

This means that we can replace the spring constant k with $m\omega^2$ in the potential $V(q)$:

$$V(q) = \tfrac{1}{2} m\omega^2 q^2.$$

According to classical mechanics, the energy of the particle can have any non-negative value E. For a given E, it will oscillate between the classical turning points $q = \pm A$ (where A is given by $E = \frac{1}{2} m\omega^2 A^2$).

In the quantum-mechanical treatment of this system, we shall as usual start by finding all the energy eigenfunctions and the corresponding eigenvalues. It then turns out that the oscillator has only bound states, and that the energy is quantized. We shall see how all the energy eigenvalues and the corresponding eigenfunctions can be found.

We start by writing the time-dependent Schrödinger equation on **dimensionless form,** as

$$\frac{d^2\psi(x)}{dx^2} + (\epsilon - x^2)\psi(x) = 0. \tag{T3.27}$$

Here we have introduced the dimensionless variables x and ϵ for for respectively the position and the energy:

$$x \equiv \frac{q}{\sqrt{\hbar/m\omega}} \qquad \text{and} \qquad \epsilon \equiv \frac{E}{\frac{1}{2}\hbar\omega}. \tag{T3.28}$$

We shall find the solutions of this differential equation (i.e., the energy eigenfunctions) and the corresponding energies (ϵ) using the so-called **series expansion method**.

In this method we make use of the fact that any energy eigenfunction can be expanded in terms of a Taylor series in powers of the dimensionless variable x. The coefficients in this expansion will be determined when we require that the expansion satisfies the energy eigenvalue equation (T3.23) above.

3.4.b Illustration of the series expansion method

Let us illustrate how this method works by applying it on a well-known function, the exponential function $y(x) = \exp(x)$, which has the Taylor expansion

$$y(x) = e^x = 1 + x + x^2/2! + ... = \sum_{n=0}^{\infty} \frac{x^n}{n!}.$$

This function satisfies the differential equation

$$y' = y,$$

as you can readily check. We shall now try to solve this equation using the series expansion method. We start by assuming that $y(x)$ can be expanded in an infinite power series,

$$y = \sum_{n=0}^{\infty} c_n x^{s+n} = c_0 x^s + c_1 x^{s+1} + \cdots.$$

Here we assume that $c_0 \neq 0$, and we must first find the lowest power, x^s, where we now pretend that s is unknown. Inserting into the differential equation ($y' - y = 0$) the above sum and the corresponding expression for its derivative,

$$\begin{aligned} y' &= \sum_{n=0}^{\infty} c_n(s+n)x^{s+n-1} = c_0\, sx^{s-1} + \sum_{n=1}^{\infty} c_n(s+n)x^{s+n-1} \\ &= c_0\, sx^{s-1} + \sum_{n=0}^{\infty} c_{n+1}(s+n+1)x^{s+n}, \end{aligned}$$

we get the following equation:

$$c_0\, sx^{s-1} + \sum_{n=0}^{\infty}[(s+n+1)c_{n+1} - c_n]x^{s+n} = 0.$$

This equation is satisfied for all x only if the coefficients in front of all the powers of x are equal to zero. Since c_0 is different from zero (by definition), we must thus require that

- $s = 0$, which means that the Taylor expansion starts with $c_0x^0 = c_0$, and that
- $c_{n+1} = \dfrac{c_n}{n+s+1} = \dfrac{c_n}{n+1}$.

The last formula is called a **recursion relation**, and implies that all the coefficients can be expressed in terms of c_0:

$$c_1 = \frac{c_0}{1}, \qquad c_2 = \frac{c_1}{2} = \frac{c_0}{1\cdot 2}, \qquad c_3 = \frac{c_2}{3} = \frac{c_0}{3!}, \quad \text{etc.}$$

Thus the series expansion is

$$y = \sum_{n=0}^{\infty} c_n x^n = c_0 \sum_{n=0}^{\infty} \frac{x^n}{n!}.$$

Here we recognize the sum as the Taylor expansion of $\exp(x)$.

3.4.c Series expansion methed applied to the oscillator eigenvalue equation

For the oscillator, we can in principle apply the same procedure. From the exercises, you probably remember that two of the solutions of the eigenvalue equation are

$$\psi_0 = C_0\, e^{-m\omega q^2/2\hbar} = C_0\, e^{-x^2/2} \qquad \text{and} \qquad \psi_1 = C_1\, q\, e^{-m\omega q^2/2\hbar} = C_1'\, x\, e^{-x^2/2}.$$

It is the tempting to "remove" a factor $\exp(-x^2/2)$ from all the solutions, by writing

$$\psi(x) = v(x)e^{-x^2/2}.$$

We do this hoping that the resulting series for the function $v(x)$ will be simpler (maybe even finite, as for the two solutions above). We find this series by applying the series expansion method to the diffential equation for $v(x)$, which is

$$v'' - 2xv' + (\epsilon - 1)v = 0.$$

[Verify that this equation follows when you insert $\psi(x) = v(x)\exp(-x^2/2)$ into the differential eqyuation (T3.23) for $\psi(x)$.] We now insert the infinite series [13]

$$v(x) = \sum_{k=0}^{\infty} a_k x^2\,, \qquad\qquad v' = \sum_{k=1} k a_k x^{k-1},$$

and

$$v'' = \sum_{k=2} k(k-1)a_k x^{k-2} = \sum_{k=0}(k+2)(k+1)a_{k+2}x^k,$$

into the above equation for $v(x)$ and get

$$\sum_{k=0}^{\infty}\left[(k+2)(k+1)a_{k+2} - (2k+1-\epsilon)a_k\right]x^k = 0.$$

This equation is satisfied (for all x) only if all the parentheses $[\cdots]$ are equal to zero. This leads to the **recursion relation**

$$a_{k+2} = a_k\,\frac{2k+1-\epsilon}{(k+1)(k+2)}, \qquad k = 0, 1, 2, \cdots. \tag{T3.29}$$

By repeated use of this relation, we can express the coefficients a_2, a_4 etc in terms of a_0, — and a_3, a_5, etc in terms of a_1. The "solution" for $v(x)$ then is

$$\begin{aligned} v(x) \;\; &= \;\; a_0\left[1 + \frac{1-\epsilon}{2!}\,x^2 + \frac{(1-\epsilon)(5-\epsilon)}{4!}x^4 + \cdots\right] \\ &\quad + a_1\left[x + \frac{3-\epsilon}{3!}\,x^3 + \frac{(3-\epsilon)(7-\epsilon)}{5!}x^5 + \cdots\right], \end{aligned}$$

where you should now be able to write down the next term for both of the two series.

If these two (supposedly infinite) series do not *terminate*, we see from the recursion relation that the ratio between neighbouring coefficients will go as

$$\frac{a_{k+2}}{a_k} \simeq \frac{2}{k}$$

for large k. As shown in Hemmer, this is the same ratio as in the expansion of $x^p e^{x^2}$, where x^p is an arbitrary power of x. This means that $\psi(x) = v(x)\exp(-x^2/2)$ will for large $|x|$ behave as $\exp(+x^2/2)$ multiplied by some power of x. Such a function will approach infinity in the limits $x \to \pm\infty$, and *that* is not allowed for an eigenfunction. The only way to avoid this unacceptable behaviour is if the series *terminate*, so that $v(x)$ becomes a **polynomial.** On the other hand, when both series terminate, $\psi(x) = v(x)\exp(-x^2/2)$ becomes a normalizable function. (This is related to the fact that the energy spectrum is discrete, as we shall see.)

Let us investigate then under what conditions the series terminate. We start by considering the case in which ϵ is *not* an odd integer, $\epsilon \neq 1, 3, 5, 7, \cdots$. Then neither of the two series terminate. In order to avoid a diverging solution, we must then set $a_0 = a_1 = 0$, which gives $v(x) \equiv 0$, so that $\psi(x)$ becomes the trivial "null" solution. The conclusion

[13] Here, we are simply assuming that the lowest power in the Taylor series for $v(x)$ is a constant, a_0, as is the case for the ground state.

is that the differential equation does not have any acceptable solution (and that $\widehat{H}$ does not have any eigenfunction) for $\epsilon \neq 1, 3, 5, 7, \cdots$. We must therefore look more closely into what happens when ϵ *is* an odd integer (equal to $1, 3, 5, 7$, etc):

For

$$\epsilon = 1, 5, 9, \cdots = \underline{2n+1 \qquad (\text{with} \quad n = 0, 2, 4, \cdots)},$$

we see that the *first* of the two series terminates (but not the second one). To get an acceptable eigenfunction, we must then get rid of the second series by setting $a_1 = 0$. We note that this makes $v(x)$ a polynomial of degree n. For $\epsilon = 5$, e.g., which corresponds to $n = 2$, we see that the polynomial is of degree 2, with only *even* powers of x. Then also the eigenfunction $\psi_n(x) = v_n(x)\exp(-x^2/2)$ is an even function of x (symmetric).

For

$$\epsilon = 3, 7, 11, \cdots = \underline{2n+1 \qquad (\text{with} \quad n = 1, 3, 5, \cdots)},$$

it is the *second* series that terminates, and we have to set $a_0 = 0$. Then $v(x)$ becomes a polynomial with only *odd* powers of x, and $\psi_n(x) = v_n(x)\exp(-x^2/2)$ is an antisymmetric eigenfunction.

In both cases, the energy eigenvalues are given by

$$\boxed{E_n = \tfrac{1}{2}\hbar\omega \cdot \epsilon = (n + \tfrac{1}{2})\hbar\omega,} \qquad n = 0, 1, 2, \cdots. \tag{T3.30}$$

With these results we have finally proved the formula for the (non-degenerate) energy spectrum of the harmonic oscillator, and also the symmetry properties of the wave functions, which were announced early in this course.

It is now a simple matter to find the polynomials $v_n(x)$ by inserting $\epsilon = 1, 3, 5$ etc in the formula above. It is customary to normalize these polynomials $v_n(x)$ in such a way that the highest power is $2^n x^n$. These polynomials are known as the **Hermite polynomials**, $H_n(x)$. In section 3.5.3 in Hemmer, and in section 4.7 in B&J, you can find a number of useful formulae for the Hermite polynomials. One of these formaulae is

$$\int_{-\infty}^{\infty} H_n^2(x) e^{-x^2} dx = 2^n n! \sqrt{\pi}.$$

This can be used to show that the *normalized* energy eigenfunctions, expressed in terms of the position variable q, are

$$\boxed{\psi_n(q) = \left(\frac{m\omega}{\pi\hbar}\right)^{1/4} \frac{1}{\sqrt{2^n n!}}\, e^{-m\omega q^2/2\hbar}\, H_n\left(\frac{q}{\sqrt{\hbar/m\omega}}\right),} \tag{T3.31}$$

where

$$\begin{aligned} H_0(x) &= 1, \\ H_1(x) &= 2x, \\ H_2(x) &= 4x^2 - 2, \qquad \left(x = q\sqrt{m\omega/\hbar}\right) \\ H_3(x) &= 8x^3 - 12x, \\ H_4(x) &= 16x^4 - 48x^2 + 12, \quad \text{etc.} \end{aligned}$$

A few simple exercises:

3.1 Show that the next polynomial is $H_5(x) = 32\,x^5 - 160\,x^3 + 120\,x$.
3.2 What are the expectation values $\langle\, x \,\rangle_{\psi_n}$ for the eigenfunctions $\psi_n(x)$?
3.3 What happens with the energy levels if we increase the particle mass by a factor 4?
3.4 What happens with the energy levels if we increase the spring constant k in the potential $V(x) = \frac{1}{2}kx^2$, that is, if we make the potential more "narrow"?
3.5 It can be shown that the non-hermitian operators

$$\widehat{a} = \sqrt{\frac{m\omega}{2\hbar}}\,q + \frac{i\widehat{p}}{\sqrt{2m\hbar\omega}} = \sqrt{\frac{m\omega}{2\hbar}}(q + \frac{\hbar}{m\omega}\frac{\partial}{\partial q}) \quad \text{og} \quad \widehat{a}^\dagger = \sqrt{\frac{m\omega}{2\hbar}}(q - \frac{\hbar}{m\omega}\frac{\partial}{\partial q})$$

have the properties

$$\widehat{a}\psi_n(q) = \sqrt{n}\,\psi_{n-1}(q) \qquad \text{og} \qquad \widehat{a}^\dagger\psi_n(q) = \sqrt{n+1}\,\psi_{n+1}(q).$$

Check that these operators act as they should for $n = 0$, that is, that they give $\widehat{a}\psi_0 = 0$ and $\widehat{a}^\dagger\psi_0 = \psi_1$.

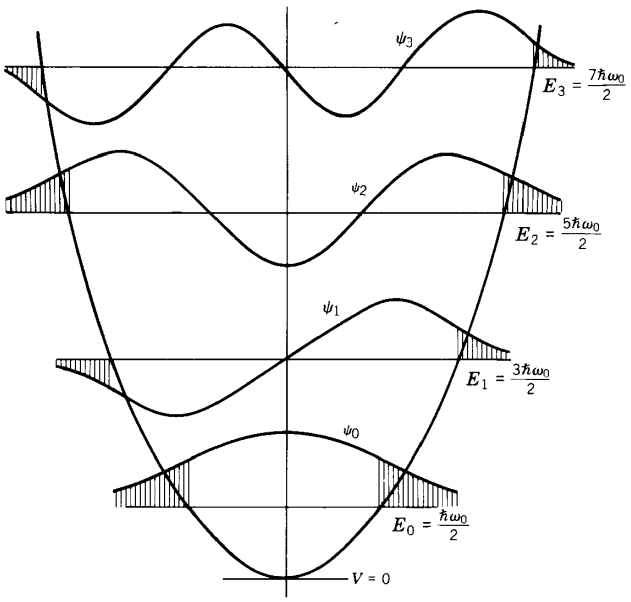

The figure shows the first four energy eigenfunctions. The hatched areas indicate where the eigenfunctions "penetrate" into the respective classically forbidden regions (beyond the classical turning points). Note also that ψ''/ψ changes sign at the turning points: *Between* the turning points the eigenfunctions curve *towards* the x axis. In the "forbidden" regions they curve *away* from the axis. This is in accordance with the eigenvalue equation

$$\psi''/\psi = x^2 - \epsilon = x^2 - 2n - 1,$$

which tells us that the turning points occur for

$$q\sqrt{m\omega/\hbar} = x = \pm\sqrt{\epsilon} = \pm\sqrt{2n+1}.$$

In Hemmer, or in B&J, you can as mentioned study the wonderful properties of the Hermite polynomials more closely. You can also find a section on the comparison with the classical harmonic oscillator:

3.4.d Comparison with the classical harmonic oscillator

In hemmer, you can observe that there is a certain relationship between the probability density for an energy eigenfunction $\psi_n(q)$ and the *classical* probability density for a particle that oscillates back and forth with the energy E_n. The classical probability density is largest near the classical turning points, where the particle's velocity is lowest. For large quantum numbers, the quantum mechanical probability density of course has a large number of zeros, but apart from these local variations, we notice that the local maxima are largest close to the turning points.

At the same time, there is a fundamental difference between the classical oscillatory behavour and the quantum-mechanical behaviour of the probability density for a stationary state. The latter *is* really stationary; it does not move, contrary to the classical motion of the particle, which we are used to observe macroscopically. Thus the classical motion must correspond to a non-stationary solution of the time-dependent Schrödinger equation for the oscillator. Such a solution can be found p 59 in Hmmer:

Suppose that a harmonic oscillator (a particle with mass m in the potential $V(q) = \frac{1}{2}m\omega^2 q^2$) is prepared in the initial state

$$\Psi(q,0) = \left(\frac{m\omega}{\pi\hbar}\right)^{1/4} e^{-m\omega(q-q_0)^2/2\hbar},$$

at $t = 0$, which is a wave function with the same *form* as the ground state, but centered at the position q_0 instead of the origin. As we have seen in the exercises, the expectation values of the position and the momentum of this initial state are $\langle\, q \,\rangle_0 = q_0$ and $\langle\, p \,\rangle_0 = 0$. Furthermore, the uncertainty product is "minimal":

$$\Delta q = \sqrt{\frac{\hbar}{2m\omega}}, \qquad \Delta p = \sqrt{\frac{\hbar m\omega}{2}}, \qquad \Delta q \Delta p = \tfrac{1}{2}\hbar.$$

The solution of the Schrödinger equation for $t > 0$ can always be written as a superposition of stationary states for the oscillator,

$$\Psi(q,t) = \sum_n c_n \psi_n(q) e^{-iE_n t/\hbar}.$$

By setting $t = 0$ in this expansion formula we see (cf Tillegg 2) that the coefficient c_n is the projection of the initial state $\Psi(q,0)$ onto the eigenstate $\psi_n(q)$:

$$c_n = \langle\, \psi_n, \Psi(0) \,\rangle \equiv \int_{-\infty}^{\infty} \psi_n^*(q)\Psi(q,0)dq.$$

By calculating these coefficients and inserting them into the expansion formula, it is possible to find an explicit formula for the time-dependent wave function. This formula is not very transparent, but the resulting formula for the probability density is very simple:

$$|\Psi(q,t)|^2 = \left(\frac{m\omega}{\pi\hbar}\right)^{1/2} e^{-m\omega(q-q_0\cos\omega t)^2/\hbar}.$$

We see that this has the same Gaussian form as the probability density of the initial state, only centered at the point $q_0\cos\omega t$, which thus is the expectation value of the position at the time t:

$$\langle\, q \,\rangle_t = q_0 \cos\omega t.$$

Furthermore, the *width* of the probability distribution stays constant, so that the uncertainty Δq keeps the value it had at $t = 0$. The same turns out to be the case for the uncertainty Δp, and hence also for the uncertainty product $\Delta q \Delta p$, which stays "minimal" the whole time. Thus, in this particular state we have a wave packet oscillating back and forth in a "classical" manner, with constant "width". Admittedly, the position is not *quite* sharp, and neither is the energy. However, if we choose macroscopic values for the amplitude q_0 and/or the mass m, then we find that the relative uncertainties, $\Delta q/q_0$ and $\Delta E/\langle E \rangle$, become negligible. Thus, in the macroscopic limit the classical description of such an oscillation agrees with the quantum-mecnical one. This means that classical mechanics can be regarded as a limiting case of quantum mechanics.

3.4.e Examples

In Nature is there is an abundance of systems for which small deviations from equilibrium can be considered as harmonic oscillations. As an example, we may consider a particle moving in a one-dimensional potential $V(q)$, with a stable equilibrium at the position q_0. If we expand $V(q)$ in a Taylor series around the value q_0, then the derivative is equal to zero at the equilibrium position $[V'(q_0) = 0]$, so that

$$\begin{aligned} V(q) &= V(q_0) + (q - q_0)V'(q_0) + \frac{1}{2!}(q - q_0)^2 V''(q_0) + \cdots, \\ &= V(q_0) + \tfrac{1}{2}k(q - q_0)^2 + \cdots \qquad [\text{with } k \equiv V''(q_0)]. \end{aligned}$$

As indicated in the figure on the next page, $V(q)$ will then be approximately harmonic (parabolic) for small displacements from the equilibrium position; [14]

$$V(q) \approx V(q_0) + \tfrac{1}{2}k(q - q_0)^2 \equiv V_h(q) \qquad (\text{for small } |q - q_0|).$$

In this approximation, the energy levels become equidistant,

$$E_n^{\mathrm{h}} = V(q_0) + \hbar\omega(n + \tfrac{1}{2}), \qquad n = 0, 1, 2, \cdots, \qquad \omega = \sqrt{k/m} = \sqrt{V''(q_0)/m},$$

and the energy eigenfunctions are the same as those found in section **3.4.c** above, only displaced a distance q_0. As an example, the ground state in this approximation is

$$\psi_0^{\mathrm{h}}(q) = \left(\frac{m\omega}{\pi\hbar}\right)^{1/4} e^{-m\omega(q-q_0)^2/2\hbar}.$$

[14] We suppose that $V''(q_0) > 0$.

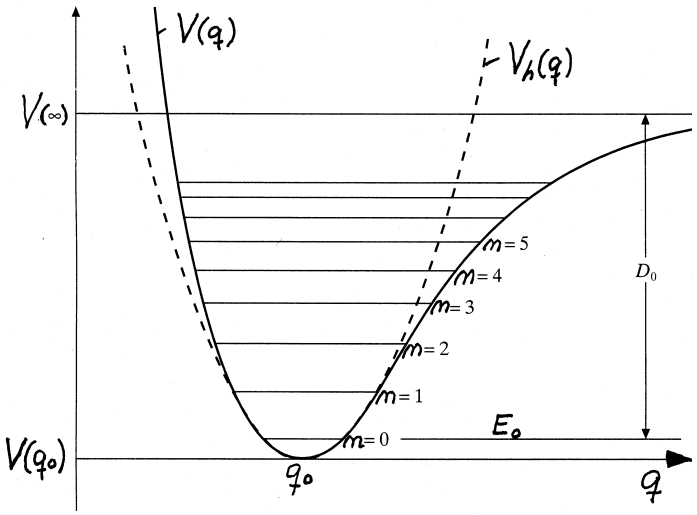

We can expect the "harmonic" results E_n^{h} (for the energy) and $\psi_n^{\mathrm{h}}(q)$ (for the corresponding energy eigenfunction) to be fairly close to the exact results E_n and $\psi_n(q)$, provided that the parabola $V_h(q)$ does not deviate too much from the real potential $V(q)$ in the region where the probability density $|\psi_n(q)|^2$ differs significantly from zero; that is, the particle must experience that the force is by and large harmonic.

The "real" potential $V(q)$ in the figure is meant to be a model of the potential energy that can be associated with the vibrational degree of freedom for a two-atomic molecule. (Then q is the distance between the two nuclei, and q_0 is the equilibrium distance.) For small and decreasing q, we see that the potential increases faster than the parabola. The molecule resists being compressed, because this "causes the two electronic clouds to overlap".

For $q > q_0$, we see that the molecule also strives against being "torn apart", but here we observe that the potential does not increase as fast with the distance as $V^{\mathrm{h}}(q)$. While the force according to the harmonic approximation increases as $|F| = dV^{\mathrm{h}}/dq = m\omega^2 q$, we see that the real force pretty soon starts to decrease. For sufficiently large distances it in fact approaches zero, in such a way that it costs a finite amount of energy $D_0 = V(\infty) - E_0$ to tear the molecule apart (when it initially is in the ground state). This is the so-called **dissociation energy**.

For the lowest values of n, for which $V(q)$ and $V_h(q)$ are almost overlapping between the turning points, the harmonic approximation will be good, and the energy levels will be almost equidistant. For higher n, for which the potential $V(q)$ is more "spacious" than the parabolic $V_h(q)$, the levels will be more closely spaced than according to the harmonic approximation, as indicated in the figure. This can also be understood using curvature arguments: With more space at disposal, the wave function $\psi(q)$ can have more zeros (higher n) for a given energy.

The distance between neigbouring vibrational energy levels for two-atomic gases like e.g. O_2 typically is of the order of $0.1 - 0.2$ eV, which is much larger than the energies needed to excite the rotational degree of freedom ($10^{-4} - 10^{-3}$ eV). In statistical physics one learns that the probability of finding the molecule excited e.g. to the first vibrational level ($n = 1$) is negligible when $k_B T << \hbar\omega$, that is, when the temperature T is much lower than

$$\frac{\hbar\omega}{k_B} \sim \frac{0.1 \text{ eV}}{8.6 \cdot 10^{-5} \text{ eV/K}} \sim 10^3 \text{ K}.$$

By measuring emission lines from a hot gas we find one spectral line for each transition between neighbouring energy levels. This is because there is the so-called **selection rule** $\Delta n = \pm 1$ for transitions between vibrational states. A measurement of the line spectrum thus gives us the energy differences beteen all neighbouring levels. These spectra are in reality a little bit more complicated by the fact that the emitted photon carries away an angular momentum $\pm\hbar$. This means that the change of vibrational energy is accompanied by a change of the angular momentum, and hence also of the rotational energy. Thus what we are dealing with really are **vibrational-rotational spectra**.

For molecules with more than two atoms, the motion becomes more complicated. The molecule can be sujected to stretching, bending, torsion, etc. However, all such complicated motions can be analyzed in terms of so-called **normal modes**, which can be treated as a set of independent oscillators.

The same can be said about solids like a crystal. Here, each normal mode corresponds to a standing wave with a certain wavelength an a certain frequency. For the mode with the highest frequencies (shortest wavelengths), only a small number of atoms are oscillating "in step"; for long wavelengths large portions of the crystal are oscillating "in phase".

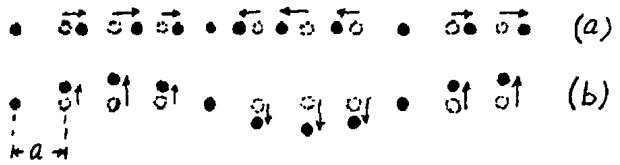

Longitudinal (a) and transverse (b) modes with wavelength $8a$ in a one-dimensional mono-atomic crystal. The arrows show the displecements from the equilibrium posistions.

Here too the normal modes are defined in such a way that they can be treated as a set of independent harmonic oscillators. But the number of modes is so large that the frequency spectrum will be practically continuous. (Cf the discussion of black-body radiation in Tillegg 1.)

In some cases, e.g. for sound waves, we can treat such oscillations classically. In other cases, e.g. for a crystal which has been cooled down to a very low temperature ($T \gtrsim 0$), the quantum number of each "oscillator" will be small; perhaps even zero, so that only a few of the oscillators are excited. We must then treat the system quantum mechanically, and take into account that energy is exchanged in the form of quanta $\hbar\omega$. So here we are dealing with quantized sound waves.

A similar set of standing waves occurs when we consider electromagnetic waves in a cavity. In some cases (e.g. in the microwave oven), these waves can be treated classically. Each standing wave is then treated with the mathematics of a classical harmonic oscillator. But certain properties of cavity radiation can only be understood if these oscillators are quantized, as Planck and Einstein discovered well over a hundred years ago. It is the quantization of the electromagnetic modes of radiation which leads to the **photon description** of the electromagnetic field. In this description, a mode of frequency ω and energy $E_n = \hbar\omega(n + \frac{1}{2})$ contains n photons with energy $\hbar\omega$ (in addition to the "zero-point energy" $\frac{1}{2}\hbar\omega$).

In a similar way, the quantization of the crystal' "oscillators" leads to the concept of **phonons** (sound quanta), which are analoguous to the photons.

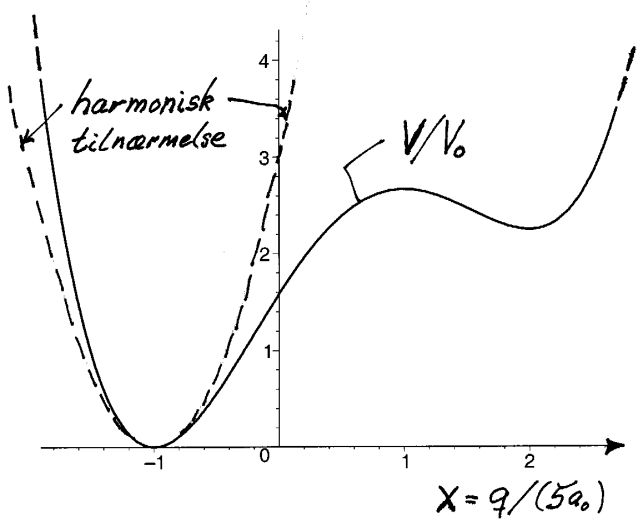

Exercise:

An electron is moving in the potential

$$V(q) = V_0 \left[\frac{x^4}{4} - \frac{2x^3}{3} - \frac{x^2}{2} + 2x + \frac{19}{12} \right], \qquad \text{where} \qquad x \equiv \frac{q}{5a_0} \quad \text{and} \quad V_0 = \frac{6\hbar^2}{m_e a_0^2}.$$

Here, a_0 is the Bohr radius, so that $V_0 = 12 \cdot \hbar^2/(2m_e a_0^2) = 12 \cdot 13.6$ eV $= 12$ Rydberg. The potential has a minimum for $x = x_0 = -1$ (i.e. for $q = q_0 = -5a_0$).

a. Check this by calculating dV/dq and d^2V/dq^2 at the minimum.

b. Show that the energy of the ground state is $E_0 \approx V_0/10$, if you apply the "harmonic approximation" (see the figure).

c. Add the "energy line" E_0 to the diagram. Do you think that the result for E_0 is reasonably accurate compared to the *exact* value of the ground-state energy for the potential V?

3.5 Free particle. Wave packets

(Griffiths)

3.5.a Stationary states for a free particle

In classical mechanics the free particle (experiencing zero force) is the simplest thing we can imagine: cf Newton's 1. law. Quantum mechanically, however, even the free particle represents a challenge, as pointed out by Griffiths on pages 44–50.

We consider a free particle in one dimension, corresponding to $V(x) = 0$. For this case it is very easy to solve the time-independent Schrödinger equation,

$$\widehat{H}\,\psi(x) = E\,\psi(x),$$

which takes the form

$$\frac{d^2\psi}{dx^2} = -k^2\,\psi, \qquad \text{with} \quad k \equiv \frac{1}{\hbar}\sqrt{2mE}.$$

As solutions of this equation we may use $\sin kx$ and $\cos kx$ (which we remember from the discussion of the one-dimensional box, also called the infinite potential well), but here we shall instead use $\exp(\pm ikx)$.

These solutions also emerge if we start out with the harmonic waves

$$\psi_p(x) = (2\pi\hbar)^{-1/2}\, e^{ipx/\hbar}, \tag{T3.32}$$

which are eigenfunctions of the momentum operator $\widehat{p}_x$: Since

$$\widehat{p}_x\psi_p(x) = p\,\psi_p(x),$$

we have

$$\widehat{H}\,\psi_p(x) = \frac{\widehat{p}_x^2}{2m}\,\psi_p(x) = \frac{p^2}{2m}\,\psi_p(x).$$

Thus, the momentum eigenfunction $\psi_p(x)$ also is an energy eigenfunction (for the free particle) with energy E, if we choose either of the two p values

$$p = \pm\sqrt{2mE} = \pm\hbar k.$$

So, no matter how we start out, we may conclude that for the free particle in one dimension there are two unbound energy eigenstates for each energy $E > 0$ (degeneracy 2). For $E = 0$, we have only one solution, $\psi = (2\pi\hbar)^{-1/2} =$ constant. Thus the energy *spectrum* is $E \in [0, \infty)$. This means that the complete set $\psi_p(x)$ of momentum eigenstates also constitutes a complete set of egenstates of the free-particle Hamiltonian $\widehat{H} = \widehat{p}_x^2/2m$. The corresponding stationary solutions,

$$\boxed{\Psi_p(x,t) = \psi_p(x)\, e^{-i(p^2/2m)t/\hbar}, \qquad (E = p^2/2m),} \tag{T3.33}$$

is also a complete set.

3.5.b Non-stationary states of a free particle

Since the momentum eigenstates $\psi_p(x)$ require delta-function normalization (see, e,g, 2.4.4 in Hemmer), none of the stationary states $\Psi_p(x,t)$ above can represent a physically realizable state, stricly speaking. A pysical state has to be localized (quadratically integrable), and hence can not be stationary for a free particle. The time-dependent wave function $\Psi(x,t)$ of such a physical state can be found once the initial state $\Psi(x,0)$ is specified, in the following way:

(i) $\Psi(x,t)$ may always be written as a superposition of the stationary states $\Psi_p(x,t)$ (because this set is complete):

$$\Psi(x,t) = \int_{-\infty}^{\infty} \phi(p)\,\Psi_p(x,t)dp. \tag{T3.34}$$

[Here, the function $\phi(p)$ plays the role as expansion coefficient.]

(ii) Setting $t = 0$ we have

$$\Psi(x,0) = \int_{-\infty}^{\infty} \phi(p)\,\psi_p(x)dp.$$

This means that $\phi(p)$ is the projection of the initial state $\Psi(x,0)$ on $\psi_p(x)$,

$$\phi(p) = \langle\, \psi_p, \Psi(0) \,\rangle \equiv \int_{-\infty}^{\infty} \psi_p^*(x)\Psi(x,0)dx,$$

and this function may be calculated when $\Psi(x,0)$ is specified.

(iii) Inserting the resulting coefficient function $\phi(p)$ into the integral for $\Psi(x,t)$ and calculating this integral, we will find how $\Psi(x,t)$ behaves as a function of t. This method will be applied in an exercise, to study the behaviour of free-particle wave packets.

3.5.c Phase velocity. Dispersion

Even if we *do not* specify $\Psi(x,0)$, it is possible to study some general properties of the free-particle wave function

$$\Psi(x,t) = \int_{-\infty}^{\infty} \phi(p)\, \Psi_p(x,t)\, dp. \tag{T3.35}$$

First, we note that $\Psi_p(x,t)$ has the form

$$e^{i(px-Et)/\hbar} = e^{i(kx-\omega t)},$$

with

$$k = \frac{p}{\hbar} \qquad \text{and} \qquad \omega = \frac{E}{\hbar} = \frac{\hbar k^2}{2m}. \tag{T3.36}$$

Digression: Electromagnetic waves in vacuum

Let us digress and for a moment consider electromagnetic waves in vacuum ($\omega = c|\mathbf{k}|$). A monochromatic wave propagating in the x direction then is described essentially by the harmonic wave function

$$e^{i(kx-\omega t)} = e^{ik(x-ct)},$$

or rather by the real part of this, $\cos k(x-ct)$. The wave crests move with the velocity

$$v_f = \frac{\omega}{k} = c.$$

This so-called **phase velocity** is independent of the wave number k; in vacuum waves with different wavelengths all move with the same (phase) velocity c:

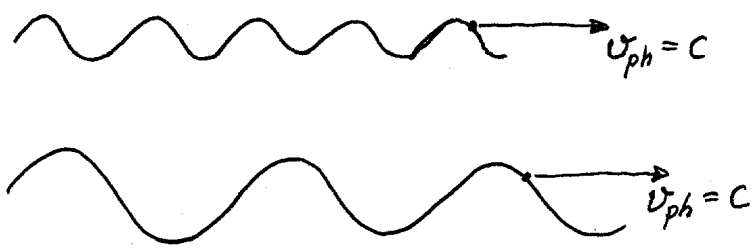

By superposing such plane harmonic waves with different wavelengths, we can make a **wave packet**,

$$f(x,t) = \int_{-\infty}^{\infty} \phi(k)\, e^{i(kx-\omega t)} dk = \int_{-\infty}^{\infty} \phi(k)\, e^{ik(x-ct)} dk. \tag{T3.37}$$

Since each component wave in this superposition is moving with the same velocity c, we realize that the resulting *sum* (the integral) of these component waves will also move with the velocity c and with *unchanged form*.

This can also be verified using the formula above. If we name the wave function at $t = 0$,

$$f(x,0) = \int_{-\infty}^{\infty} \phi(k)\, e^{ikx} dk$$

by $g(x)$, we see from the right-hand side of (T3.37) that

$$f(x,t) = g(x - ct) :$$

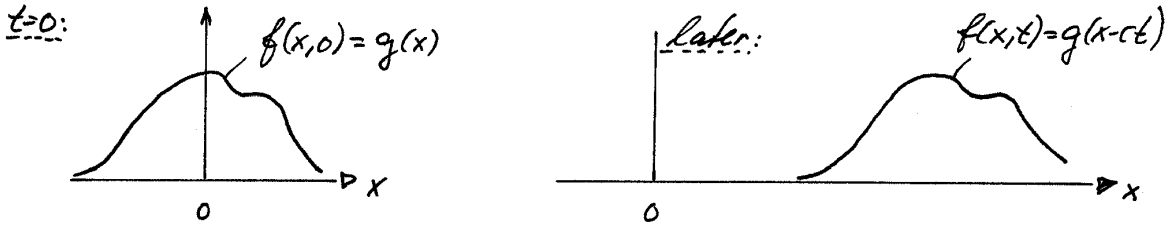

This is illustrated in the figure, where the diagram on the left shows the wave function at $t = 0$. In the figure on the right, at time t, we find the same wave form, shifted to the right by the amount ct.

Thus, a plane electromagnetic wave packet propagates with unchanged form in vacuum. We note that this is because the phase velocity $v_f = \omega/k = c$ in vacuum is independent of k.

In an optical fiber, on the other hand, the phase velocity depends slightly on the wavelength. The harmonic component waves then propagate with slightly different velocities. As a result, a wave packet will *change form* during propagation. For example, if we start with a *sharp* pulse (corresponding to a **broad band** of wavelengths), the pulse will typically be spread out during propagation. This is called **dispersion**, and this is the reason for calling

$$\omega = \omega(k)$$

the **dispersion relation** for the medium in question.

3.5.d Group velocity

After this digression, let us see what we can learn from the dispersion relation

$$\omega = \frac{\hbar}{2m}\, k^2$$

for the harmonic free-particle wave (the de Broglie wave)

$$\Psi_p(x,t) = \psi_p(x) e^{-i(p^2/2m)t/\hbar} \;\propto\; e^{i(kx-\omega t)}.$$

We note that the phase velocity of this harmonic wave,

$$v_f = \frac{\omega}{k} = \frac{\hbar k}{2m} = \frac{p}{2m},$$

comes out as the classical velocity p/m divided by 2. There is no reason to worry about this result. Neither the phase velocity nor the phase itself of the de Broglie wave are observable. And the same can be said about the phases of all other qauntum-mechanical wave functions that we encounter. In this respect, there is an essential difference between the quantum-mechanical wave functions and classical waves like e.g. an ocean wave.

We also note that the phase velocity of the de Broglie wave depends strongly on the wave number ($\propto k$). In order to find out what this means, we can make a wave packet

$$\Psi(x,t) = \int_{-\infty}^{\infty} \phi(k)\, e^{i(kx-\omega t)} dk, \qquad\qquad \omega = \omega(k), \tag{T3.38}$$

where we consider a fairly sharp distribution $\phi(k)$ of wave numbers, around a central value k_0. This corresponds to an equally sharp momentum distribution around a central value $p_0 = \hbar k_0$:

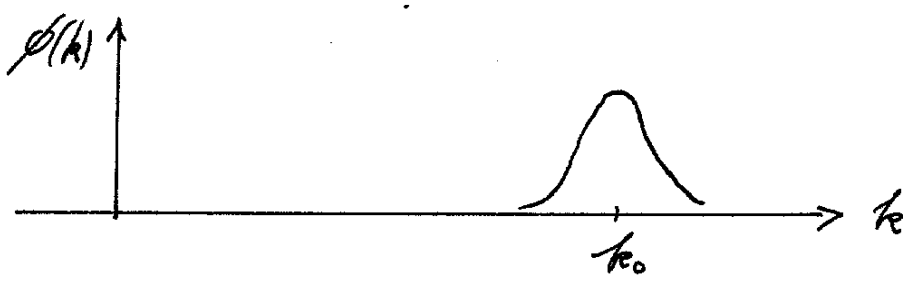

Thus we suppose that the width (Δk) of this distribution is relatively small. It is the relevant to consider the Taylor expansion of $\omega(k)$ around the central value k_0,

$$\omega(k) = \omega(k_0) + (k-k_0)\left.\frac{d\omega}{dk}\right|_{k_0} + \frac{1}{2!}(k-k_0)^2 \left.\frac{d^2\omega}{dk^2}\right|_{k_0} .$$

In this case, there are no higher-order terms in the expansion, because ω goes as k^2. We find

$$\begin{aligned} \omega(k_0) &= \frac{\hbar}{2m}\, k_0^2 \equiv \omega_0, \\ \left.\frac{d\omega}{dk}\right|_{k_0} &= \frac{\hbar}{m}\, k_0 \equiv v_g, \\ \left.\frac{d^2\omega}{dk^2}\right|_{k_0} &= \frac{\hbar}{m}. \end{aligned}$$

With this notation the exact expansion of $\omega(k)$ around k_0 is

$$\omega(k) = \omega_0 + v_g(k-k_0) + \frac{\hbar}{2m}(k-k_0)^2. \tag{T3.39}$$

Since we consider a rather narrow distribution $\phi(k)$, the last term in this expression will be relatively small. Let us therefore neglect this term and try to use the approximation

$$\omega(k) \approx \omega_0 + v_g(k-k_0). \tag{T3.40}$$

Inserting this into the integral for $\Psi(x,t)$, and moving the factors which are independent of the integration variable k outside the integral, we find that

$$\begin{aligned}\Psi(x,t) &\approx \int_{-\infty}^{\infty} \phi(k)\, e^{i(kx-[\omega_0+v_g(k-k_0)]t)} dk \\ &= e^{-i\omega_0 t} e^{ik_0 v_g t} \int_{-\infty}^{\infty} \phi(k)\, e^{ik(x-v_g t)} dk. \end{aligned} \tag{T3.41}$$

For $t = 0$ this simplifies to

$$\Psi(x,0) = \int_{-\infty}^{\infty} \phi(k)\, e^{ikx} dk \equiv g(x).$$

Inspired by the digression above, we denote the last integral by $g(x)$. Comparing with the last integral in (T3.41), we then see that the latter is $g(x - v_g t) = \Psi(x - v_g t, 0)$. Thus, essentially without doing any explicit calculations, we have found that the approximation $\omega \approx \omega_0 + v_g(k - k_0)$ leads to the result

$$\Psi(x,t) \approx e^{-it(\omega_0 - k_0 v_g)}\, \Psi(x - v_g t, 0). \tag{T3.42}$$

Apart from the irrelevant phase factor, we see that the wave packet has the same form as for $t = 0$; it has only moved a distance $v_g t$ during the time t. This means that the quantity $v_g \equiv d\omega/dk|_{k_0}$ introduced above is the velocity of the wave packet or wave "group". Thus we may state the following rule:

A wave packet or wave group with a narrow distribution $\phi(k)$ of wave numbers centered around k_0 will move with the **group velocity**

$$v_g = \left.\frac{d\omega}{dk}\right|_{k_0}. \tag{T3.43}$$

In the case at hand, with the dispersion relation $\omega = \hbar k^2/2m$, we find the group velocity

$$v_g = \frac{\hbar k_0}{m}. \tag{T3.44}$$

We note that this is the classical velocity of a particle with momentum $p_0 = \hbar k_0$, which corresponds to the central Fourier component in the wave packet.

We also note that the neglection of the quadratic term in the expansion

$$\omega(k) = \omega(k_0) + (k - k_0) \left.\frac{d\omega}{dk}\right|_{k_0} + \frac{1}{2!}(k - k_0^2) \left.\frac{d^2\omega}{dk^2}\right|_{k_0}$$

corresponds to the neglection of the dispersion of the wave packet. If the quadratic term is included (corresponding here to the use of the exact dispersion relation $\omega(k) = \hbar k^2/2m$), one finds that the wave packet changes form during the propagation.

If one chooses a very narrow distribution $\phi(k)$ (small $\Delta p_x = \hbar \Delta k$), corresponding to a very long wave packet (large Δx), then it will take a long time before the dispersion shows up.

In the opposite case, if one insists on a very *short* wave packet in x-space (small Δx), then this requires a very *broad* distribution of wave numbers (large $\Delta p_x = \hbar \Delta k$). Then the dispersion will be much stronger, and it will show up very fast.

3.6 Scattering in one dimension

[Hemmer 3.6, B&J 4.2–4.4]

3.6.a What is scattering in one dimension?

Scattering is very often a three-dimensional process: A grain of dust scatters an incoming ray of light in all directions. And when a bat sends a sound wave against an insect, the scattered sound wave spreads over all directions, happily also backwards towards the bat. The angular distribution of the scattered wave depends in general on the form of the object, and also on the wavelength.

Scattering is used for structural investigations in many fields, on objects varying in size from macroscopic bodies, via microscopic structures, and all the way down to sub-atomic particles. As an example, the structure of a molecule can be studied by bombarding it with electrons as projectiles. The angular distribution of scattered electrons then gives us information on the structure of the molecule (the target).

Such a process must be treated quantum mechanically. One then employes a wave function consisting of a plane wave representing the incoming particles and a spherical scattered wave representing the scattered particles. Such wave functions are called scattering wave functions. The angular distribution of the scattered wave will depend on the wavelength (and hence the energy) of the projectiles.

What is scattering in one dimension? As an example, we may consider a plane sound wave incident (perpendicularly) on a plane wall. Another example is light incident on a window. Then for each photon, there are only two possible outcomes: Either transmission straight through or reflection. (We are neglecting absorption here.) This process can be treated as a one-dimensional problem, where incoming, transmitted and reflected photons are represented by plane waves propagating either forwards or backwards. Correspondingly, a beam of electrons incident perpendicularly on a metal surface will experience a potential $V(x)$ depending only on one variable. Such a process may be treated by the use of a wave function which depends only on x, and thus we have a one-dimensional scattering process.

3.6.b Scattering calculation based on energy eigenfunctions

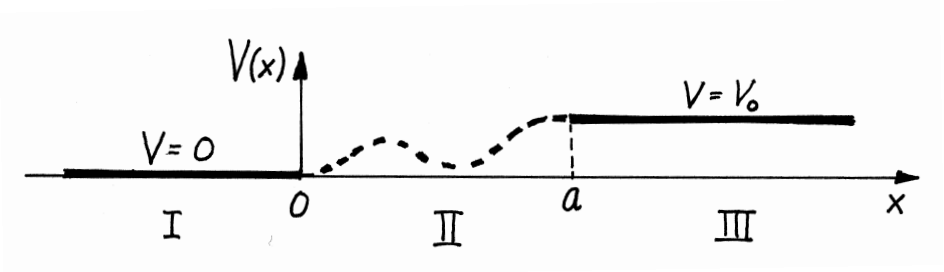

We start by considering some general properties af a scattering process where a particle incident from the left (region I in the figure, where $V(x) = 0$), meets a region II ($0 < x < a$) where the potential is unspecified (and where the force $F_x = dV(x)/dx$ differs from zero), and then is either reflected back to region I or transmitted to region II ($x > a$), where $V(x) = V_0$. Here, V_0 is ether positive, negative or equal to zero. We shall consider potentials which are also constant in region II, so that we are dealing with piecewise

constant potentials. The simplest way to deal with such scattering processes is to use energy eigenfunctions $\psi_E(x)$, which correspond to stationary solutions $\Psi_E(x,t) = \psi_E(x)e^{-iEt/\hbar}$ of the Schrödinger equation. If we limit ourselves to consider particle energies E larger than $\max(0, V_0)$, we may write down wave numbers and general solutions of the eigenvalue equation $\widehat{H}\psi_E = E\psi_E$ for regions I and III as follows:

I: $x < 0$	II: $0 < x < a$	III: $x > a$
$\psi_I = Ae^{ikx} + Be^{-ikx}$	ψ_{II} depends on the potential	$\psi_{III} = Ce^{ik'x} + De^{-ik'x}$
$k = \frac{1}{\hbar}\sqrt{2mE}$ $\left(E = \frac{\hbar^2 k^2}{2m}\right)$		$k' = \frac{1}{\hbar}\sqrt{2m(E - V_0)}$ $\left(E = V_0 + \frac{(\hbar k')^2}{2m}\right)$

(T3.45)

With an energy E larger than $\max(0, V_0)$, we have two independent energy eigenfunctions for this potential (degeneracy 2). This gives us a certain freedom in the choice of the form of this wave function. We use this freedom to choose to set the coefficient D equal to zero. The reason is that the remaining term $Ce^{ik'x}$ in region III, combined with the time factor $e^{-iEt/\hbar}$, describes particles moving to the right, i.e., transmitted particles with a positive group velocity (cf the discussion of the group velocity above). The discarded term $De^{-ik'x}e^{-iEt/\hbar}$ would correspond to particles with a negative group velocity in region III, and such particles should not occur in this problem. To the right of the point $x = a$ there is no force which can cause particles to turn around and come back towards the left.

Thus, we have a picture where particles are sent in from the left (represented by the incoming wave $Ae^{ikx} \equiv \psi_i$). Some of these (represented by the transmitted wave $Ce^{ik'x} \equiv \psi_t$) are transmitted to the right, while others (represented by the reflected wave $Be^{-ikx} \equiv \psi_r$) are reflected back to the left. We may call the condition $D = 0$ a boundary condition. Note that this condition gives us an asymmetric wave function (also if the potential $V(x)$ should happen to be symmetric).

Current densities

In order to find the probabilities of reflection and transmission, we use the formula

$$j(x) = \Re\mathrm{e}\left[\psi^* \frac{\hbar}{im}\frac{\partial\psi}{\partial x}\right] \tag{T3.46}$$

to calculate the current densities in regions I and III. It is easy to find the transmitted current density $j_t = j_{III}$, since the wave function in this region is simply $\psi_{III} = Ce^{ik'x}$:

$$j_t = j_{III} = \Re\mathrm{e}\left[C^* e^{-ik'x}\frac{\hbar}{im}C(ik')e^{ik'x}\right] = \underline{\underline{|C|^2\frac{\hbar k'}{m}}} = |\psi_{III}|^2 v'. \tag{T3.47}$$

(Note that the current density comes out as the product of the density and the group velocity.)

Before going on to calculate the current in region I, we note that the incoming wave $\psi_i = Ae^{ikx}$ and the reflected wave $\psi_r = Be^{-ikx}$, if either of them were alone in region I, would give current densities which we may denote by

$$j_i = |A|^2 \frac{\hbar k}{m} \qquad \text{and} \qquad j_r = |B|^2 \frac{\hbar(-k)}{m}, \tag{T3.48}$$

respectively. We note that the latter is negative, directed to the left. When we do the calculation properly, taking into account that *both* these waves are present in region I, we find that the current density in region I is the algebraic sum of j_i and j_r:

$$\begin{aligned} j_I &= \Re\mathrm{e}\left[\left(A^*e^{-ikx} + B^*e^{ikx}\right)\frac{\hbar k}{m}\left(Ae^{ikx} - Be^{-ikx}\right)\right] \\ &= |A|^2\frac{\hbar k}{m} + |B|^2\frac{\hbar(-k)}{m} + \Re\mathrm{e}\left[AB^*e^{2ikx} - A^*Be^{-2ikx}\right]\frac{\hbar k}{m} \\ &= j_i + j_r = j_i - |j_r|. \end{aligned} \tag{T3.49}$$

Here, we have used that

$$\Re\mathrm{e}[z - z^*] = \Re\mathrm{e}[2i\Im\mathrm{m}(z)] = 0.$$

We shall see below that

$$j_I = j_{III} (= j_{II}), \tag{T3.50}$$

and that the current density is in general independent of x for a stationary state in a one-dimensional potential $V(x)$, which is the case here. Therefore, (T3.49) may also be written as

$$j_i = |j_r| + j_I = |j_r| + j_t. \tag{T3.51}$$

This relation tells us that the probability is **conserved**; the incoming current is split in two, a reflected current (moving towards the left) and a transmitted current (moving to the right). The probabilities of reflection and transmission then must be

$$R = \frac{|j_r|}{j_i} \qquad \text{and} \qquad T = \frac{j_t}{j_i}. \tag{T3.52}$$

Thus the relation

$$R + T = 1 \tag{T3.53}$$

is an expression of probability conservation.

This indicates that the key formula (T3.50) has to do with probability conservation. We can verify this by noting that for a stationary state $\Psi(x,t) = \psi(x)e^{-iEt/\hbar}$ in one dimension, the probability density $\rho = |\Psi(x,t)|^2 = |\psi(x)|^2$ is time independent. From the continuity equation $\boldsymbol{\nabla}\cdot\mathbf{j} + \partial\rho/\partial t = 0$, which here takes the form

$$\frac{\partial j}{\partial x} = -\frac{\partial \rho}{\partial t} = 0,$$

it thus follows that the current density $j(x)$ is x-independent:

$$j(x) = \text{constant}, \qquad \text{(for a stationary state in one dimension)}. \tag{T3.54}$$

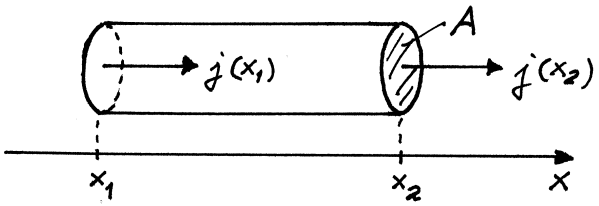

This can also be understood from the figure above: Because the probability density $\rho(x)$ is time independent, there can be no change in the amount of probability inside the volume between x_1 and x_2. Therefore, the current entering the volume, $Aj(x_1)$, must be equal to the current leaving it, $Aj(x_2)$, for arbitrary x_1 and x_2.

In order to proceed, and find the values of

$$R = \frac{|j_r|}{j_i} = \left|\frac{B}{A}\right|^2 \qquad \text{and} \qquad T = \frac{j_t}{j_i} = \left|\frac{C}{A}\right|^2 \frac{k'}{k}, \tag{T3.55}$$

one must of course specify the potential inside region II (depending on the forces acting inside this region). When this part of the potential is known, it is in principle possible to find the general solution of $\widehat{H}\psi_E = E\psi_E$ for this region (containing two undetermined coefficients, F and G). By using the continuity conditions for ψ and ψ' for $x = 0$ and $x = a$, one can then find the ratios B/A and C/A (and also F/A and G/A). This means that the complete eigenfunction $\psi_E(x)$ is known, except for a normalization constant (A). However, the over-all normalization constant is not needed in this kind of problem. Only the ratios B/A and C/A count, and we may very well choose to work e.g. with $A = 1$.

3.6.c Scattering treated with wave packets

Before applying the above method on concrete examples, it may be instructive to show how such a scattering process can be understood in terms of wave packets. An incident particle with reasonably well-defined energy can be represented by a wave packet which is a superposition of stationary solutions of the type we have seen above. Let us first recapitulate how such a wave packet behaves for a free particle (zero potential). Superposing free-particle stationary solutions $e^{i(kx-\omega t)}$ we can construct a wave packet

$$\Psi_R(x,t) = \int \phi(k) e^{i(kx-\omega t)} dk, \qquad \omega = \hbar k^2/2m. \tag{T3.56}$$

With a suitable distribution $\phi(k)$ around a central value k_0, corresponding to the energy $E = \hbar^2 k_0^2/2m$,

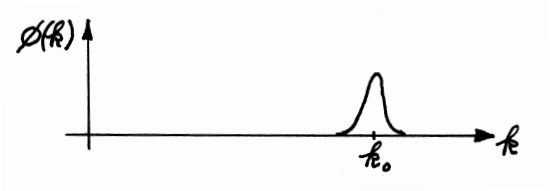

we can construct a normalized wave packet $\Psi_R(x,t)$ moving to the right (R for right), with a position

$$\langle\, x \,\rangle_R = \frac{\hbar k_0}{m}\, t.$$

This packet passes the origin at $t = 0$.

In the same manner, we can use the plane waves $e^{i(-kx-\omega t)}$ to make a packet

$$\Psi_L(x,t) = \int \phi(k) e^{i(-kx-\omega t)} dk, \tag{T3.57}$$

with the same distribution $\phi(k)$ as above. This integral is the same as for $\Psi_R(x,t)$, only with $-x$ instead of x. Hence the packet

$$\Psi_L(x,t) = \Psi_R(-x,t) \tag{T3.58}$$

is simply the mirror image of $\Psi_R(x,t)$; it is moving towards the *left* (L) and passes the origin at $t = 0$. Here we should note that $\Psi_R(x,t)$ differs (significally) from zero only in a fairly small region around $\langle x \rangle_R$, and correspondingly for the mirror image $\Psi_L(x,t)$. The first figure below illustrates the two packets for $t < 0$,

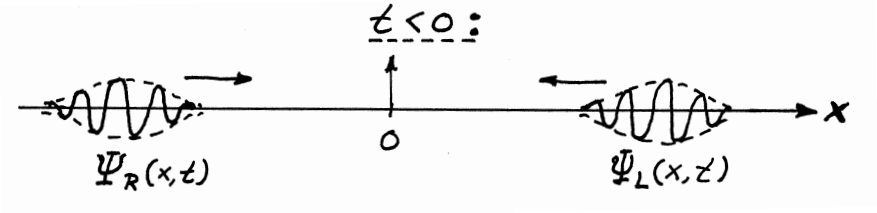

and the second one shows the situation for $t > 0$:

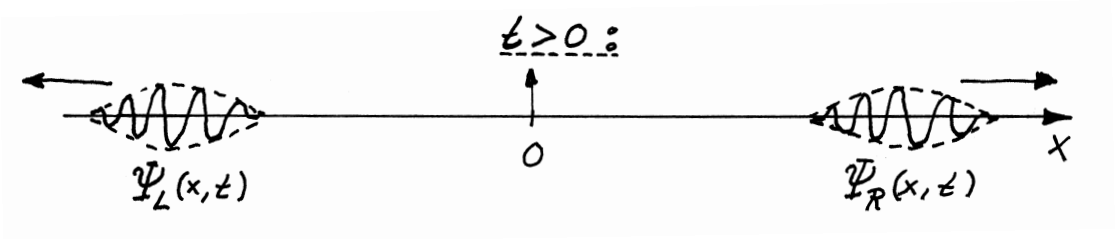

Both these packets are solutions of the time-dependent Schrödinger equation for the free particle and are moving with constant group velocities (cf Newton's first law). Note also that the Schrödinger equation preserves the normalization of the packets (even if the *form* changes somewhat due to the dispersion).

Let us now turn to the scattering problem in section **b**. For simplicity, we suppose that $V_0 = 0$, so that $V(x) = 0$ both for $x < 0$ and $x > a$. With $A = 1$ the stationary solution in **b** then takes the form

$$\Psi_E(x,t) = \begin{cases} e^{i(kx-\omega t)} + Be^{i(-kx-\omega t)} & \text{for} \quad x < 0 \qquad (\omega = E/\hbar = \hbar k^2/2m), \\ Ce^{i(kx-\omega t)} & \text{for} \quad x > a. \end{cases} \tag{T3.59}$$

Superposing such stationary solutions with the same distribution $\phi(k)$ that was used above for the free particle, we find a solution of the time-dependent Schrödinger equation for the potential $V(x)$ on the form [15]

$$\Psi(x,t) = \int \phi(k)\Psi_E(x,t)dk = \begin{cases} \Psi_R(x,t) + B\Psi_L(x,t) & \text{for} \quad x < 0, \\ C\Psi_R(x,t) & \text{for} \quad x > a. \end{cases} \tag{T3.60}$$

[15] In the integrals in (T3.60), the coefficients $B/A = B$ and $C/A = C$ in reality are energy dependent; they depend on the integration variable k. But in view of the rather sharp distribution $\phi(k)$ the k-dependence will be so slow that we can neglect it and move $B(k) \approx B(k_0) \equiv B$ and $C(k) \approx C(k_0) \equiv C$ outside the respective integrals, as we have done in (T3.60).

To realize how this wave function behaves for large negative t or large positive t, we only need to remember the behaviour of the free-particle packets $\Psi_R(x,t)$ and $\Psi_L(x,t)$, keeping in mind that positive and negative x must be treated separately, according to the formula above.

Let us first look at the situation for large negative t: We remember that Ψ_R then differs from zero only in a limited region far out to the left, while Ψ_L is far out to the right. Thus for $x < 0$, equation (T3.60) tells us that we have only Ψ_R moving in from the left, while for $x > a$ we have nothing. For large negative t (and also for large positive t), it can also be shown that $\Psi(x,t)$ is equal to zero in region II, for $0 < x < a$. Thus the situation is as follows:

large negative t:

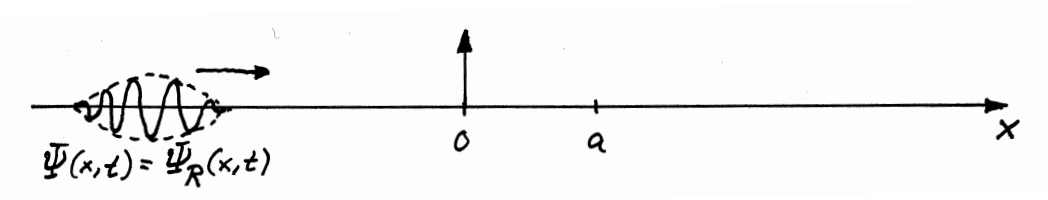

Since Ψ_R is normalized, it follows that the wave function $\Psi(x,t)$ is normalized for large negative t. But then it is normalized for *all* t, because the Schrödinger equation preserves the normalization, as we have already stated.

Proceeding then to the situation for large positive t, we remember that Ψ_R then has moved far out to the right, while the mirror image Ψ_L is equally far out to the left. From (T3.60) it then follows that for $x < 0$ we have only $B\Psi_L$ moving outwards on the negative x-axis. For $x > 0$ we have only $C\Psi_R$ on its way out to the right.

large positive t:

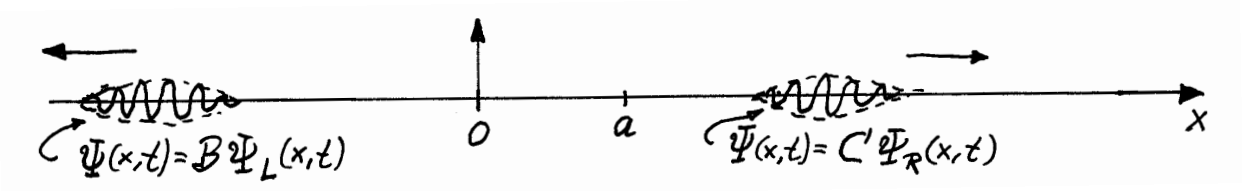

Thus the incoming wave packet has been divided in two, a reflected wave $B\Psi_L(x,t)$ and a transmitted wave $C\Psi_R(x,t)$.

The transmission and reflection coefficients are now obviously given by the probabilitity contents in the respective packets for large positive t. The transmission coefficient is given by the probability in the transmitted packet, that is, by the integral

$$T = \int |\Psi(x,t)|^2 dx = |C|^2 \int |\Psi_R(x,t)|^2 dx = |C|^2, \qquad \text{(T3.61)}$$

where the only contributions come from the region for large positive x where the transmitted wave is now found. In the same way we find the reflection coefficient

$$R = \int |\Psi(x,t)|^2 dx = |B|^2 \int |\Psi_L(x,t)|^2 dx = |B|^2, \tag{T3.62}$$

where the integral goes over the packet Ψ_L which is now far out on the left. As we see, the results of this wave-packet consideration agree with those found in the preceeding section using only the energy eigenfunction $\psi_E(x)$ (for the special case $k' = k$, and with $A = 1$).

Comments:

(i) While the wave packet is *divided*, each individual particle must choose between being reflected or transmitted. Quantum mechanics gives us only the probabilities, and can not tell us what happens with a given particle. The theory gives statistical predictions.

(ii) The term De^{-ikx} which was discarded from $\psi_E(x)$ for $x > a$, would have given a wave packet incident from the right (for negative t). Such an *action* can not be *caused* by projectiles incident from the left. *That* would violate the law of **cause and action**, it would **violate causality**, as we use to say.

(iii) To find the size of R and T one must, as in section **b**, specify $V(x)$ for region II and find the eigenfunction $\psi_E(x)$ for all x, including the coefficients B and C. When $\psi_E(x)$ has been found for all x, it is in principle possible to find the behaviour of the wave-packet solution $\Psi(x,t)$ also for t around zero, that is, the behaviour of the packet just when it "divides" in two. This behaviour is in general quite complicated.

(iv) Even if the wave-packet method gives a simple physical picture of the scattering process, we see that the results are completely equivalent to those found using the *simpler method* in section **b**. In the examples below we shall therefore use the eigenfunction method. We start by considering scattering by a step potential.

3.6.d Scattering by a step potential

The step potential can model e.g. the potential experienced by an electron close to the surface of a metal. The figure to the left illustrates a realistic potential. On the right this has been replaced by our simpler model potential, a piecewise constant potential, for which the calculation is easier.

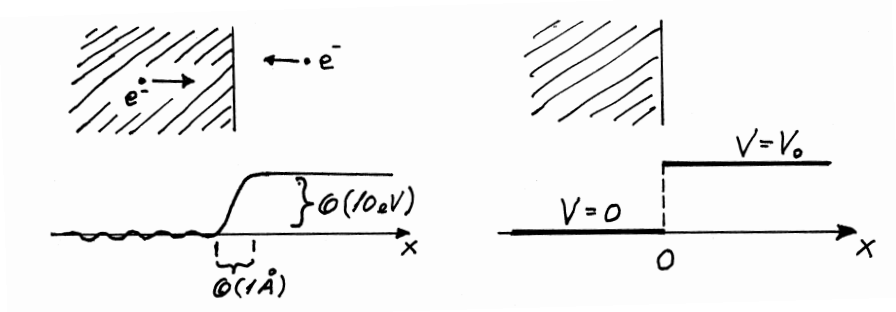

We consider first

1. Particle incident from the left, with $E > V_0$

Classically, a particle with $E > V_0$ will be transmitted with 100% probability. It only changes velocity, because the kinetic energy is smaller on the right.

In quantum mechanics, we have just learnt that the behaviour of the particle can be analyzed using an energy eigenfunction $\psi_E(x)$. In the two regions this function has the forms

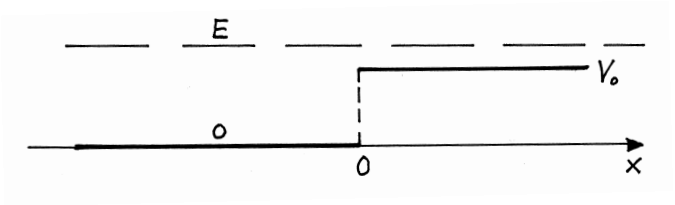

I: $x < 0$	II: $x > 0$
$\psi_I = e^{ikx} + re^{-ikx}$	$\psi_{II} = te^{ik'x}$
$\psi_I' = ik(e^{ikx} - re^{-ikx})$	$\psi_{II}' = ik'te^{ik'x}$
$k = \frac{1}{\hbar}\sqrt{2mE}$ $\left(E = \frac{\hbar^2k^2}{2m}\right)$	$k' = \frac{1}{\hbar}\sqrt{2m(E-V_0)}$ $\left(E = V_0 + \frac{(\hbar k')^2}{2m}\right)$
$j_I = j_i + j_r = 1 \cdot \frac{\hbar k}{m} + \lvert r\rvert^2 \cdot \frac{-\hbar k}{m}$	$j_{II} = j_t = \lvert t\rvert^2 \frac{\hbar k'}{m}$
$R = \frac{\lvert j_r\rvert}{j_i} = \lvert r\rvert^2$	$T = \frac{j_t}{j_i} = \lvert t\rvert^2 \frac{k'}{k}$

Here we denote the coefficients by r and t instead of B and C. We have used the results from section **b** to write down expressions for the density currents and the reflection and transmission coefficients. (Note that we have excluded a term $De^{-ik'x}$ from the general solution for region II; cf the discussion in section **b**).

We shall proceed to determine the coefficients r and t using the continuity of ψ and ψ' for $x = 0$. This gives

$$(1) \qquad 1 + r = t \qquad \text{and}$$

$$(2) \qquad 1 - r = t \cdot \frac{k'}{k} \qquad (\text{follows from } ik - ikr = ik't)\,.$$

Addition and subtraction of (1) and (2) gives

$$2 = t(1 + k'/k) \implies t = \frac{2k}{k + k'}$$

$$2r = t(1 - k'/k) \implies r = \frac{k - k'}{k + k'}.$$

Thus,

$$\boxed{R = |r|^2 = \left(\frac{k - k'}{k + k'}\right)^2 \qquad \text{and} \qquad T = |t|^2\frac{k'}{k} = \frac{4kk'}{(k + k')^2}.} \tag{T3.63}$$

Here we see that quantum mechanics gives a certain probability of reflection ($R \neq 0$) for all $E > V_0$, contrary to classical mechanics. Our calculation shows quite clearly that this non-classical reflection is due to the wave nature of the particles, inherent in the Schrödinger equation. (Note that the potential step corresponds to a force opposite to the initial direction of motion, corresponding to an "up-hill". Howver, in this case force times distance (the step size) is smaller than the initial kinetic energy, and then the particle is only slowed down; it does not turn around, according to classical mechanics.

Reciprocity

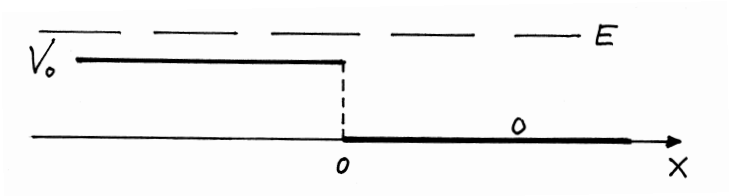

If we turn the potential around, still letting the particle be incident from the left, we only need to interchange k and k' in the calculation above. This does not change the results for R and T. (Thus we still have non-classical reflection, although the particle now encounters a "down-hill", corresponding to a force along the incident direction of motion.)

We can conclude that the partial reflection of the wave on the preceeding page (and hence of the wave packet) happens — not because the particles meet a region with higher V — but because they experience a *steep change* of the potential, with a corresponding change in the wavelength.

The fact that R and T are "invariant" under the interchange of k and k' is characteristic for all waves. In optics this property is known as **reciprocity**. As you may have noticed, the formulae are the same as for other types of waves, e.g. for light incident perpendicularly on on an air-glass surface.

R as a function of E/V_0

To illustrate how R depends on E/V_0 we note that

$$\frac{k'}{k} = \sqrt{(E - V_0)/E} = \sqrt{1 - V_0/E}.$$

This gives

$$R = 1 - T = \left(\frac{1 - \sqrt{1 - V_0/E}}{1 + \sqrt{1 - V_0/E}} \right)^2 \qquad (E > V_0). \tag{T3.64}$$

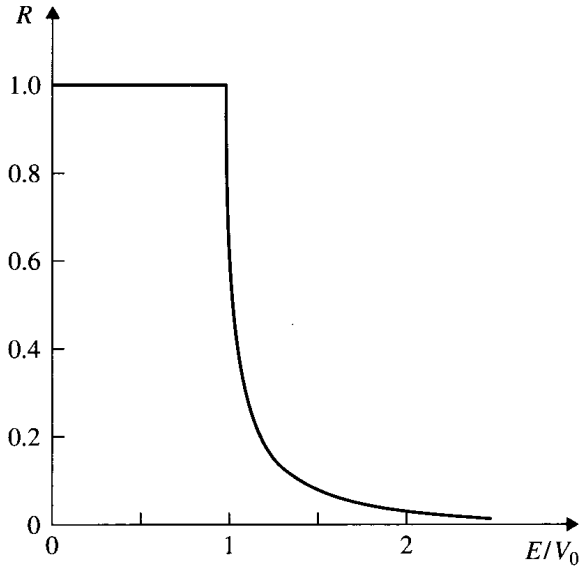

For values of E only slightly larger than V_0, we see that there is almost 100% reflection, that is, a strong deviation from the classical result. However, for increasing values of E/V_0 this deviation decreases fast, since R decreases rapidly. This is clearly illustrated in the figure above. Here we have also included the quantum-mechanical result for $E < V_0$, which agrees with the classical one: In point 2 below we show that all particles with $E < V_0$ are reflected ($R = 1$).

A paradox?

The fact that particles with $E > V_0$ are *reflected* with a certain probability is of course contrary to our "macroscopic intuition", especially when the particle meets a "down-hill" as in the figure on page 45. This even looks like a real paradox when we notice that the formula above for R is independent of the mass of the particle. Thus the formula should hold also for the car in the figure.

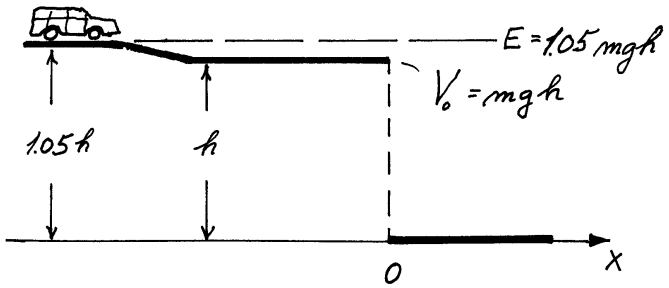

Having started by rolling down the small hill with height $0.05\,h$ the car has a kinetic energy $0.05\,mgh$ and a total energy $E = 1.05\,mgh$. This is 5% higher than the potential step ($V_0 = mgh$) corresponding to the "down-hill" with height h. According to the formula for R this should give a 45% chance for the car to be reflected, that is, for avoiding a catastrophe. But we all know that this quantum-mechanical result could cause a dangerous optimism, if believed. Experimentally, the result is catastrophic in 100 percent of the cases.

So what is wrong with this quantum-mechanical calculation? The answer lies in the model we have used for the potential step. A closer examination shows that the formula

for the reflection coefficient R is approximately correct, provided that the potential change occurs over a distance Δx which is much smaller than the wavelengths λ and λ'. This condition can perhaps be satisfied for a process on atomic scales, but for our car it is completely unrealistic. The car has a very small wavelength $\lambda = h/p = h/mv$, and Δx for the cliff will be very much larger. When the potential changes over a distance which is *much larger* than the wavelengths λ and λ', more accurate quantum-mechanical calculations show that the probability of reflection is in fact very small, not only for the car but also for small particles. This illustrates that care must be taken in the use of model potentials.

2. Particles incident from the left, with $E < V_0$

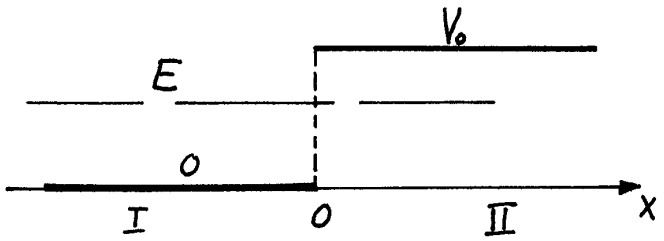

I: $x < 0$

$$\psi_I = e^{ikx} + re^{-ikx}$$

$$\psi_I' = ik(e^{ikx} - re^{-ikx})$$

$$k = \frac{1}{\hbar}\sqrt{2mE} \qquad \left(E = \frac{\hbar^2 k^2}{2m}\right)$$

II: $x > 0$

$$\psi_{II} = Ce^{-\kappa x}$$

$$\psi_{II}' = Ce^{-\kappa x}$$

$$\kappa = \frac{1}{\hbar}\sqrt{2m(V_0 - E)} \qquad \left(E = V_0 + \frac{(\hbar k')^2}{2m}\right)$$

$$j_I = j_i + j_r = 1 \cdot \frac{\hbar k}{m} + |r|^2 \cdot \frac{-\hbar k}{m} = \frac{\hbar k}{m}(1 - |r|^2)$$

$$R = \frac{|j_r|}{j_i} = |r|^2$$

What is new here is that the general solution in region II (for $x > 0$) takes the form $\psi_{II} = Ce^{-\kappa x} + De^{\kappa x}$. Here the coefficient D must be set equal to zero, because the energy eigenfunction is not allowed to diverge (for $x \to \infty$). We are thus left with the exponentially decreasing function $Ce^{-\kappa x}$ in the classically forbidden region for $x > 0$. This means that the particles penetrate a certain distance into the classically forbidden region, but not far; the **penetration depth** (where $|\psi_{II}|^2$ is reduced by a factor $1/e$) is

$$l_{\text{p.d.}} = \frac{1}{2\kappa}.$$

For large x we see that both ψ_{II} and $\rho = |\psi_{II}|^2$ approach zero. Since the particles can not accumulate anywhere for this stationary state, we realize that the number of particles

returning from the forbidden region must be equal to the number entering it. The current density then simply must be equal to zero everywhere, both inside the barrier and outside. This also follows from the fact that the current density for such a one-dimensional state is x-independent. And since j is obviously equal to zero for $x = \infty$, it must be zero for all x. This means that

$$j_I = j_i + j_r = \frac{\hbar k}{m}(1 - |r|^2) = 0,$$

that is, we have 100 % reflection, as in classical mechanics:

$$R = |r|^2 = 1.$$

This can also easily be shown by calculaion. The continuity of ψ and ψ' gives

$$\begin{aligned} (1) \qquad 1 + r &= C \qquad \text{and} \qquad ik(1 - r) = -\kappa C, \quad \text{i.e.} \\ (2) \qquad 1 - r &= i\frac{\kappa}{k} C. \end{aligned}$$

Eliminating C we find that

$$r = \frac{1 - i\kappa/k}{1 + i\kappa/k}, \quad \text{i.e.,} \quad |r| = 1, \quad \text{q.e.d.}$$

It can also be instructive to take a look at the wave function. Since $\psi_{II}/C = e^{-\kappa x}$ is real, we note that ψ_I/C must be a real linear combination of $\sin kx$ and $\cos kx$. Then it may be written as

$$\psi_I/C = A\cos(kx + \alpha) = A\cos\alpha\, \cos kx - A\sin\alpha\, \sin kx. \tag{T3.65}$$

This can also be shown in the following manner: From (1) and (2) we have

$$\begin{aligned} \psi_I/C &= \frac{1}{C}(e^{ikx} + re^{-ikx}) \\ &= \frac{1 + r}{C}\, \cos kx + i\frac{1 - r}{C}\, \sin kx \\ &= \cos kx - \frac{\kappa}{k}\, \sin kx. \end{aligned}$$

Comparing with (T3.65) we see that

$$A\cos\alpha = 1, \quad \text{dvs.} \quad A = 1/\cos\alpha \qquad \text{and} \qquad A\sin\alpha = \tan\alpha = \kappa/k.$$

Thus the result is

$$\psi_{II}/C = e^{-\kappa x} \qquad \text{and} \qquad \psi_I/C = \frac{1}{\cos\alpha}\, \cos(kx + \alpha), \quad \text{where } \alpha = \arctan\kappa/k.$$

The figure shows $\psi(x)/C$ and $|\psi(x)/C|^2$, where we note in particular that both function are smoothly joined at $x = 0$.

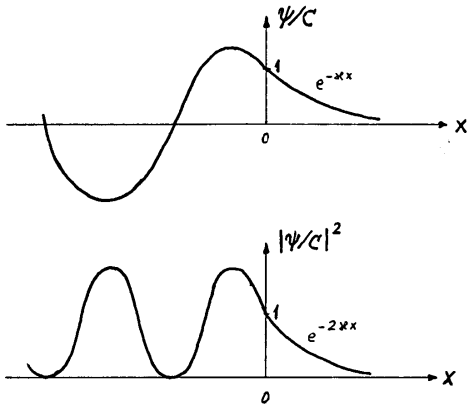

Note that the standing waves ψ and $|\psi|^2$ are sinusoidal in the allowed region to the left of the potential step. Note also the similarity with the solutions for the square well. As for the solutions for the latter, we here have stationary maxima and minima in the probability density. The difference is that here we do not have a step to the left. Therefore we do not get quantization of wavelengths and energies. Also, the sinusoidal solutions continue towards $x = -\infty$. Thus for each energy $0 < E < V_0$, we have one unbound state.

Wave-packet solution

How will a wave packet solution behave in this problem? The figure below, copied from Eisberg and Resnick, *Quantum Mechanics...*, gives a certain impression.

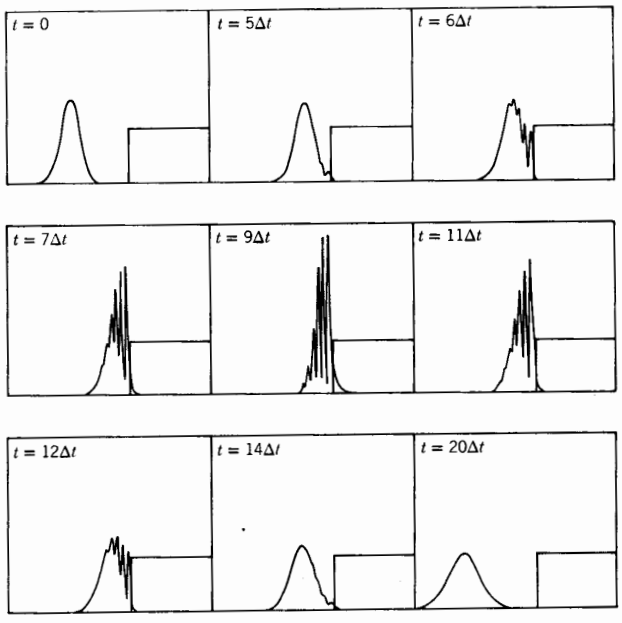

FIGURE 6-8
A potential step, and the probability density $\Psi^*\Psi$ for a group wave function describing a particle incident on the step with total energy less than the step height. As time evolves, the group moves up to the step, penetrates slightly into the classically excluded region, and then is completely reflected from the step. The complications of the mathematical treatment using a group are indicated by the complications of its structure during reflection.

Before and *after* the reflection the behaviour is as expected from our experience above. Note, however, that these graphs also include dispersion of the wave packets; the reflected wave is slightly wider than the incident one.

During the reflection process, however, the behaviour of this wave-packet solution is complicated. In addition to the penetration into the barrier, we note that the packet for $x \lesssim 0$ develops "spikes", which gradually disappear when the packet is leaving the barrier.

3.6.e Scattering on square well or square barrier

(Hemmer p 61, Griffiths p 62, B&J p 150 and p 168.)

We consider a particle with energy E incident from the left, towards the potential

$$V(x) = \begin{cases} 0 & \text{for} \quad x < 0 \quad \text{og} \quad x > L, \\ V_0 & \text{for} \quad 0 < x < L. \end{cases} \tag{T3.66}$$

(i) For $\underline{V_0 < 0}$, this is scattering on a potential well:

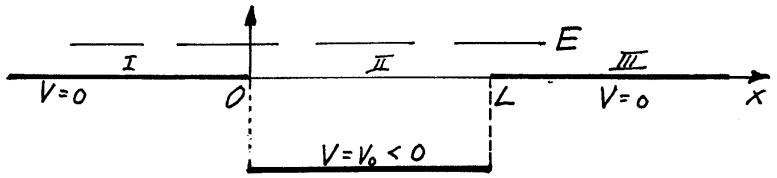

(ii) For $\underline{V_0 > 0}$ it is scattering on a potential *barrier*:

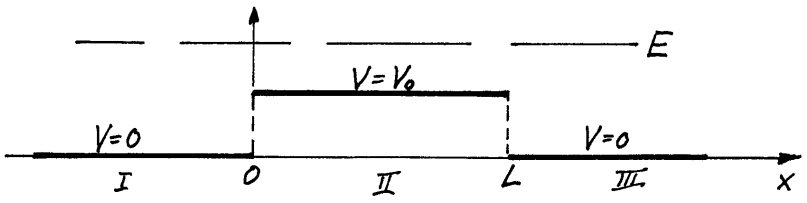

Classically the velocity in region II changes in both cases. Here the kinetic energy is $E - V_0$, but as long as V_0 is less than E, we have of course complete transmission. *Quantum mechanically* we must expect non-classical reflection even for $E > V_0$, as we are used to for other types of waves in similar situations.

(iii) The third case is when $\underline{V_0 > E}$:

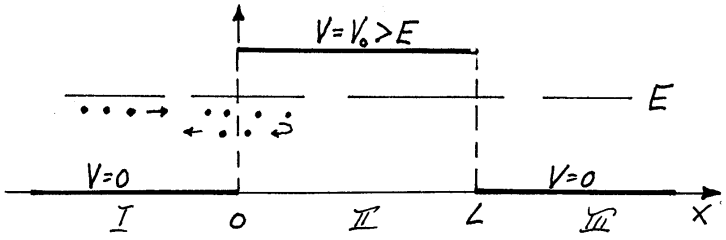

Quantum mechanically, we realize from our experience with the potential step that particles incident from the left will penetrate at least some distance into the barrier. And if the length L and the difference $V_0 - E$ are not too large, we also realize that some of the particles may

penetrate sufficiently far into the barrier that they can escape to the right. *Classically* a particle with energy $E < V_0$ can not pass the barrier. To do that, it would have to "dig a tunnel *through* the barrier". Quantum mechanically, however, there is a certain chance for transmission — therefore the name **tunnel effect** for this process.

We shall now attack these three processes with the usual strategy, which is to find an energy eigenfunction for the potential in question with the correct asymptotic behaviour:

I: $x < 0$ $(V = 0)$	II: $0 < x < L$ $(V = V_0)$	III: $x > L$ $(V = 0)$
$\psi_I = e^{ikx} + re^{-ikx}$	$\psi_{II} = ae^{iqx} + be^{-iqx}$	$\psi_{III} = te^{ikx}$
$\psi_I' = ik(e^{ikx} - re^{-ikx})$	$\psi_{II}' = iqae^{iqx} - iqbe^{-iqx}$	$\psi_{III}' = ikte^{ikx}$
$k = \frac{1}{\hbar}\sqrt{2mE}$ $\left(E = \frac{\hbar^2 k^2}{2m}\right)$	(for $V_0 < E$:) $q = \frac{1}{\hbar}\sqrt{2m(E - V_0)}$ (for $V_0 > E$:) $q = i\kappa = \frac{i}{\hbar}\sqrt{2m(V_0 - E)}$	
$j_I = j_i + j_r = \frac{\hbar k}{m}(1 - \lvert r\rvert^2)$		$j_t = \lvert t\rvert^2 \frac{\hbar k}{m}$
$j_i = 1 \cdot \frac{\hbar k}{m}, \quad j_r = \lvert r\rvert^2 \frac{-\hbar k}{m}$		
$R = \frac{\lvert j_r\rvert}{j_i} = \lvert r\rvert^2$		$T = \frac{j_t}{j_i} = \lvert t\rvert^2.$

In region I, we have a solution of the same type as for the potential step, with the same expressions as before. This is the case also for region III when we set $k' = k$, so that the solution becomes $\psi_{III} = te^{ikx}$, which has the correct behaviour for large x. In region II the wave number differs from k. We have denoted it by q, as in Hemmer. For $V_0 < 0$ (case (i), well) q is *larger* than k. For $0 < V_0 < E$, (case (ii), barrier) q is *smaller* than k. For $V_0 > E$ (tunneling case, (iii)) q becomes imaginary,

$$q = \frac{1}{\hbar}\sqrt{-2m(V_0 - E)} = \frac{i}{\hbar}\sqrt{2m(V_0 - E)} \equiv i\kappa. \tag{T3.67}$$

For the last case the solution for the barrier region II may be written on the well-known form

$$\psi_{II} = ae^{-\kappa x} + be^{\kappa x}, \qquad \psi_{II}' = \kappa\left(-ae^{-\kappa x} + be^{\kappa x}\right) \qquad (V_0 > E). \tag{T3.68}$$

This shows that the formula $\psi_{II} = ae^{iqx} + be^{-iqx}$ works also for $q = i\kappa$, that is, covers all three cases.

This means that we only have to carry out the process of joining the solutions (using continuity) once, employing the last-mentioned formula for ψ_{II}. The results for case (iii) can then be obtained by inserting $q = i\kappa$ into the final results for r, t, R and T.

We carry out the joining in the following manner:

The continuity of ψ and ψ' for $x = 0$ gives:

$$\begin{aligned} (1) \qquad 1 + r &= a + b \qquad \text{and} \qquad ik - ikr = iqa - iqb, \text{ i.e.,} \\ (2) \qquad 1 - r &= \frac{q}{k}(a - b). \end{aligned}$$

The continuity of ψ and ψ' for $x = L$ gives:

$$\begin{aligned} (3) \qquad & ae^{iqL} + be^{-iqL} = t\,e^{ikL} \qquad \text{and} \qquad iqae^{iqL} - iqbe^{-iqL} = ikt\,e^{ikL}, \text{ i.e.,} \\ (4) \qquad & ae^{iqL} - be^{-iqL} = \frac{k}{q}\,t\,e^{ikL}. \end{aligned}$$

By adding and subtracting (3) and (4) we can express the coefficients a and b in terms of the coefficient t:

$$\begin{aligned} a &= \frac{q+k}{2q}\,t\,e^{ikL}e^{-iqL}, \\ b &= \frac{q-k}{2q}\,t\,e^{ikL}e^{iqL}. \end{aligned} \tag{T3.69}$$

Setting in for a and b in (1) and (2) we can then *eliminate* a and b:

$$\begin{aligned} (1) \qquad 1 + r &= t\,e^{ikL}(\cos qL - i\,\frac{k}{q}\,\sin qL), \\ (2) \qquad 1 - r &= t\,e^{ikL}(\cos qL - i\,\frac{q}{k}\,\sin qL). \end{aligned}$$

Addition of (1) and (2) now gives

$$t = e^{-ikL}\,\frac{2kq}{2kq\cos qL - i(k^2+q^2)\sin qL}, \tag{T3.70}$$

and subtraction gives

$$r = \frac{i(q^2-k^2)\sin qL}{2kq\cos qL - i(k^2+q^2)\sin qL}. \tag{T3.71}$$

Taking the absolute squares of these, we find the general formulae for the reflection and transmission coefficients:

$$R = \frac{(q^2-k^2)^2\sin^2 qL}{4k^2q^2\cos^2 qL + (k^2+q^2)^2\sin^2 qL},$$

which can also be written as

$$\boxed{R = \frac{(k^2-q^2)^2\sin^2 qL}{4k^2q^2 + (k^2-q^2)^2\sin^2 qL},} \tag{T3.72}$$

and

$$\boxed{T = \frac{4k^2q^2}{4k^2q^2 + (k^2-q^2)^2\sin^2 qL}.} \tag{T3.73}$$

Here we see that $R + T = 1$.

These formulae contain a lot of information. This is because our problem contains several variable parameters: The length L and the height V_0 of the barrier (or the depth $|V_0|$ of the well), in addition to the mass m and the energy E of the particles.

We start by noting that we get non-classical reflection ($R > 0$) for almost all V_0 values less than E. This holds both for the well and the barrier:

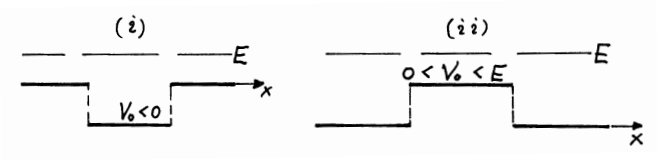

But this is of course not surprising, after our experience with scattering against a potential step. It also agrees with experience from other wave phenomena: Because the wavelength $\lambda_{II} = 2\pi/q$ differs from the wavelength $\lambda = 2\pi/k$ outside the barrier or well region, we must expect reflection.

Then it is perhaps more surprising that there are exceptions: When qL is an integer multiple of π, $qL = n\pi$ (that is, when $L = n\pi/q = n \cdot \lambda_{II}/2$ is an integer multiple of $\lambda_{II}/2$), then $\sin qL = 0$, and we find that $T = 1$ — we have *complete transmission*; the barrier or the well is "transparent" for the particles. This is analogous to a similar effect in optics, and is in a way due to destructive interference between the reflections at $x = 0$ and $x = L$. To see how this comes about, we may set $qL = n\pi$ in (T.69–71). This gives

$$r = 0, \quad t = (-1)^n e^{-ikL}, \quad a = \frac{q+k}{2q} \quad \text{and} \quad b = \frac{q-k}{2q},$$

so that the energy eigenfunction becomes:

$$\Psi_I = e^{ikx}, \qquad \psi_{II} = \frac{q+k}{2q}\, e^{iqx} + \frac{q-k}{2q}\, e^{-iqx} = \cos qx + i\,\frac{k}{q}\sin qx. \qquad \psi_{III} = (-1)^n e^{ik(x-L)} = (-1)^n \psi_I(x-L),$$

For $n = 2$ ($L = \lambda_{II}$) we see that the real part of this wave function looks like this:

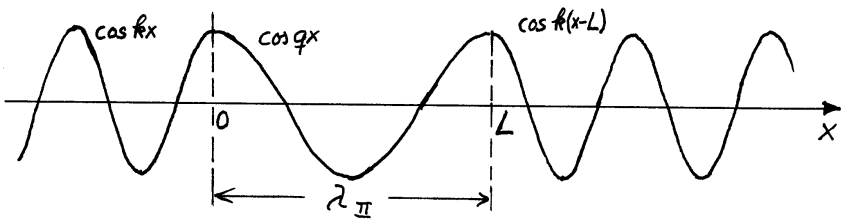

This is the same result that we get if we start with a picture of the free-particle solution e^{ikx}, "cut it in two" at $x = 0$, then move the right-hand part a distance $L = \lambda_{II}$ to the right, and insert ψ_{II} in the space between the two parts. The latter must then be chosen in such a way that ψ_{II} and ψ'_{II} are equal to ψ_I and ψ'_I for $x = 0$, and with the same values also at $x = L$. This requirement can be satisfied because ψ_{II} is periodic with wavelength λ_{II}. In this way, we may "smuggle in" a well or a barrier in such a way that it "isn't noticed".

A similar effect also occurs in three dimensions, where atoms become "transparent" or "invisible" for electrons of with certain energies. This is known as the **Ramsauer–Townsend effect**.

Between the maximal values $T = 1$ for $qL = n\pi$, the transmission coefficient has *minima*. As a function of L (with m, E and V_0 kept fixed) we see that T gets a simple periodic behaviour. This may be illustrated by two examples:

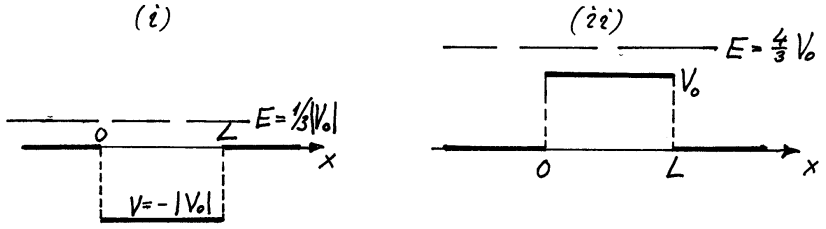

(i) Particles with energy $E = |V_0|/3$ are incident on a well with depth $|V_0|$ ($V_0 = -|V_0|$). The wave number $q_{(i)} = \sqrt{2m(E - V_0)/\hbar^2} = \sqrt{2m \cdot 4|V_0|/3\hbar^2}$ inside the well then is twice as large as the wave number $k_{(i)} = \sqrt{2m \cdot |V_0|/3\hbar^2}$ outside. Then

$$T = \frac{4k^2/q^2}{4k^2/q^2 + (k^2/q^2 - 1)^2 \sin^2 qL} = \frac{1}{1 + 9/16 \cdot \sin^2 qL}, \quad q = q_{(i)}.$$

(ii) Particles with $E = \frac{4}{3}V_0$ are incident on a barrier with height V_0. This gives $k_{(ii)} = \sqrt{2m \cdot 4V_0/3\hbar^2}$ and $q_{(ii)} = \sqrt{2m \cdot V_0/3\hbar^2}$, that is, we get the opposite ratio, $q/k = 1/2$. With this choice, we get the same T as above,

$$T = \frac{4q^2/k^2}{4q^2/k^2 + (1 - q^2/k^2)^2 \sin^2 qL} = \frac{1}{1 + 9/16 \cdot \sin^2 qL}, \quad q = q_{(ii)},$$

and we may illustrate the two results with one diagram, with qL as abscissa:

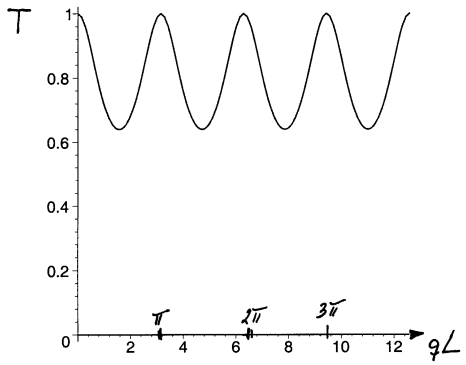

As a function of the energy E the behaviour of T is more complicated, and it is also strongly dependent of the other parameters. With $k^2 = 2mE/\hbar^2$ and $q^2 = 2m(E - V_0)/\hbar^2$ we have

$$T = \frac{4E(E - V_0)}{4E(E - V_0) + V_0^2 \sin^2 qL}, \qquad qL = \sqrt{\frac{2mL^2}{\hbar^2}(E - V_0)}. \tag{T3.74}$$

(i) As an example, we may choose a fairly "strong" well, with $V_0 = -|V_0|$ and with $\sqrt{2m|V_0|L^2/\hbar^2} \equiv \gamma = 20$. (Consulting the results for square wells, one finds that this well

allows for 7 bound states. [16] The following figure shows

$$T_{\text{brønn}} = \frac{4\frac{E}{|V_0|}(\frac{E}{|V_0|}+1)}{4\frac{E}{|V_0|}(\frac{E}{|V_0|}+1)+\sin^2 qL}, \qquad \text{with} \quad qL = \sqrt{\frac{2m|V_0|L^2}{\hbar^2}\,\frac{E-V_0}{|V_0|}} = \gamma\sqrt{\frac{E}{|V_0|}+1}, \tag{T3.75}$$

as a function of $E/|V_0|$ (brønn=well):

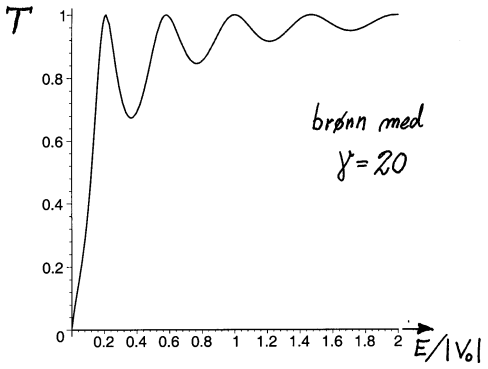

Here, you should note that T approaches zero in the limit $E \to 0$. For increasing E we observe maxima (equal to 1), each time qL is an integer multiple of $\lambda_{II}/2$). About midway between the maxima we find minima, and we note that these approach 1 for increasing energies. It is reasonable that the reflection coefficient decreases in an over-all manner like this for increasing energies. (Page 169 in B&J you will find corresponding results for a much stronger well.)

(ii) For a barrier, with $E > V_0 > 0$, the expression (T3.33) takes the form

$$T_{\text{barrier}} = \frac{4\frac{E}{V_0}(\frac{E}{V_0}-1)}{4\frac{E}{V_0}(\frac{E}{V_0}-1)+\sin^2 qL}, \qquad \text{with} \quad qL = \sqrt{\frac{2mV_0L^2}{\hbar^2}\,\frac{E-V_0}{V_0}} \equiv \gamma\sqrt{\frac{E}{V_0}-1}. \tag{T3.76}$$

In the figure below, the curve for $E/V_0 > 1$ gives the result for a barrier strength $\gamma = \sqrt{2mV_0L^2/\hbar^2} = 4$. In this region we observe a couple of maxima with aminimum in between.

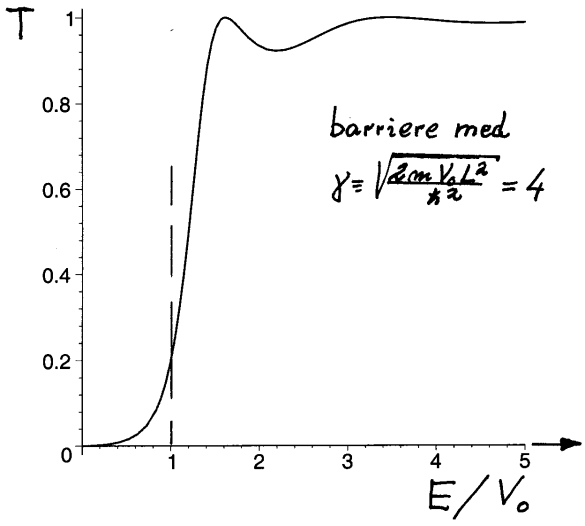

[16] Note that the parameter $\gamma = \sqrt{2m|V_0|L^2/\hbar^2}$ introduced here is twice as large as the one used in Tillegg 3, when we set $L = 2l$.

We also note that T does not go to zero when E/V_0 approaches 1 from above. Thus we have transmission even in the limit where the kinetic energy in region II goes to zero. The value of T in this limit can be found analytically by setting $E/V_0 = 1+\epsilon$ and expanding for small ϵ. The result is

$$\lim_{E\to V_0} T = \lim_{\epsilon\to 0} \frac{4\epsilon}{4\epsilon+\gamma^2\epsilon} = \frac{4}{4+\gamma^2} \quad (= 0.2 \text{ for } \gamma = 4)\,. \tag{T3.77}$$

3.6.f The tunnel effect

The above finite value of T_{barrier} in the limit $E \to V_0$ is connected to the fact that we have transmission also for $0 < E < V_0$. This is tunneling, case (iii). As you can observe in the figure, the curve for T_{barrier} connects smoothly with the probability T_{tunn} for tunneling at $E = V_0$. This is contrary to the classical probability, which jumps dicontinually, from 1 to zero. As mentioned in the discussion on page 20, we can find T_{tunn} by setting

$$q = \frac{1}{\hbar}\sqrt{2m(E-V_0)} = \frac{i}{\hbar}\sqrt{2m(V_0-E)} \equiv i\kappa$$

in the calculations above, including the general formula (T3.74) for T. With

$$\sin qL = \sin(i\kappa L) = \frac{e^{-\kappa L} - e^{\kappa L}}{2i} = i\,\sinh(\kappa L)$$

we have from (T3.74):

$$T_{\text{tunn}} = \frac{4\frac{E}{V_0}(1-\frac{E}{V_0})}{4\frac{E}{V_0}(1-\frac{E}{V_0}) + \sinh^2\kappa L}, \qquad \kappa L = \frac{L}{\hbar}\sqrt{2m(V_0-E)} \equiv \gamma\sqrt{1-E/V_0}. \tag{T3.78}$$

For $\gamma = \sqrt{2mV_0L^2/\hbar^2} = 4$, this formula gives the curve for $0 < E/V_0 < 1$ in the diagram above. Even with such a modest barrier ($\gamma = 4$), we see that T_{tunn} decreases rapidly for decreasing energy, and goes towards zero when $E \to 0$.

The central aspect of the tunnel effect is the way in which T_{tunn} depends on the barrier strength. This dependence is of course contained in the formula above. To gain a more qualitative understanding of this, we may return to the potential step, corresponding to an infinitely long barrier, $L = \infty$. The figure shows $|\psi/C|^2 = e^{-2\kappa x}$ for the case $E = 0.98\,V_0$, which gives a fairly large penetration depth $l_{\text{p.d.}} = 1/2\kappa$ into the forbidden region. (The abscissa in the figure is x in units of $l_{\text{p.d.}}$.)

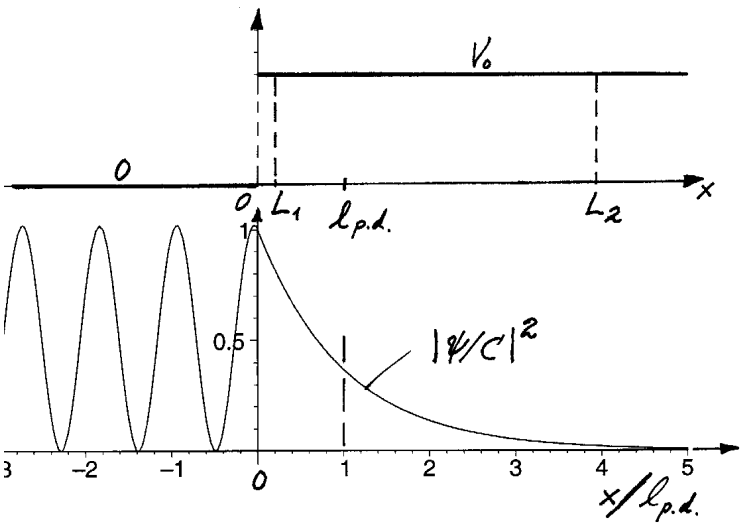

If we "cut" the infinite barrier at $x = L_1 << l_{\text{p.d.}}$, we realize that the particles will easily penetrate the resulting narrow barrier of length L_1. We must then expect that the transmission coefficient is close to 100 %. This is verified by the formula for T. When $\kappa L << \kappa l_{\text{p.d.}} = \frac{1}{2}$, we have that $\sinh^2 \kappa L \approx (\kappa L)^2 << 1$, and we find that

$$T_{\text{tunn}} \approx \frac{4\frac{E}{V_0}(1-\frac{E}{V_0})}{4\frac{E}{V_0}(1-\frac{E}{V_0})+(\kappa L)^2} \lessapprox 1, \qquad (\kappa L << 1). \tag{T3.79}$$

The opposite extreme is to cut the barrier at $x = L_2 >> l_{\text{p.d.}}$. Then $e^{-2\kappa L_2} = e^{-L_2/l_{\text{p.d.}}} << 1$. From the figure we would then naively expect to find a very small transmission probability, of the order of $e^{-2\kappa L_2}$. Also this is verified by the formula for T: For $\kappa L >> \kappa l_{\text{p.d.}} = \frac{1}{2}$ we find that

$$\sinh \kappa L = \frac{e^{\kappa L} - e^{-\kappa L}}{2} \approx \tfrac{1}{2} e^{\kappa L}$$

is very large, and (T3.78) gives a T that goes as $e^{-2\kappa L}$, as expected:

$$T_{\text{tunn}} \approx 16\frac{E}{V_0}(1-\frac{E}{V_0})\, e^{-2\kappa L} << 1, \qquad \kappa L = L\sqrt{2m(V_0-E)/\hbar^2} >> 1. \tag{T3.80}$$

Here, the slowly varying prefactor $16\frac{E}{V_0}(1-\frac{E}{V_0})$ has the maximal value 4. This prefactor is much less important than the factor $e^{-2\kappa L}$, which shows that the probability for tunneling is very sensitive to the size of the barrier, via the product κL.

The reason that the simple arguments above — based on $|\psi|^2$ for the potential step — work so well qualitatively, is that the probability density $|\psi|^2$ for the tunneling case in the barrier region $0 < x < L$ resembles very strongly $|\psi|^2_{\text{pot.}-\text{sprang}} = |Ce^{-\kappa x}|^2$ for the potential step. This is illustrated in the figure below, where we have chosen a modest barrier with a strength $\gamma = \sqrt{2mV_0L^2/\hbar^2} = 2.5$, and $E = \frac{1}{2}V_0$ (so that $\kappa = k$).

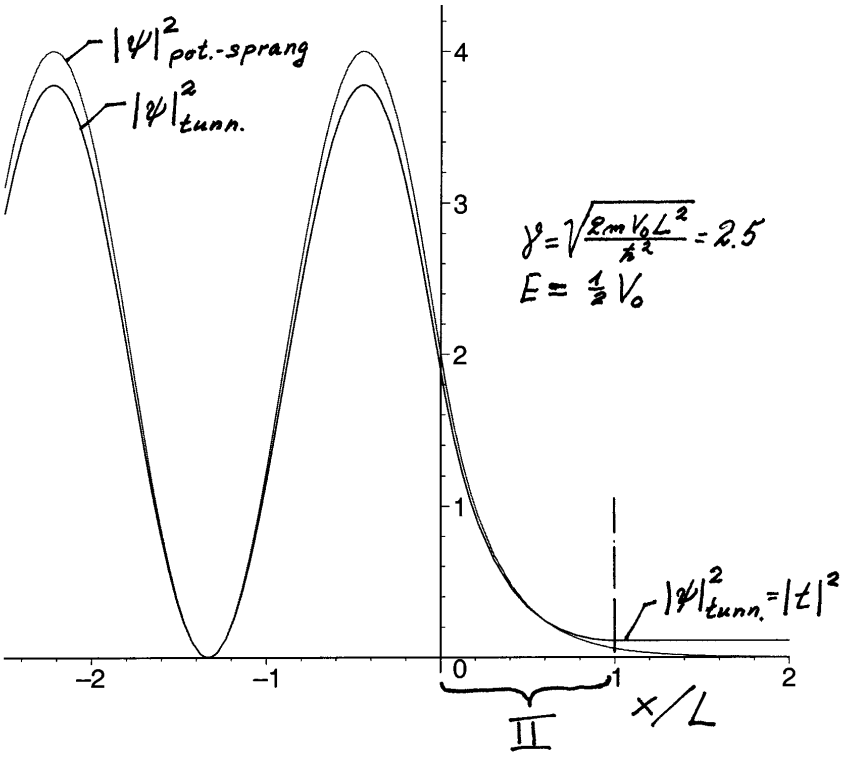

For $x > L$, $|\psi|^2_{\text{tunn}} = |te^{ikx}|^2 = |t|^2$ is constant (flat) as we see. From this part of the figure we may then read out $T_{\text{tunn}} = |t|^2$, which in this case is about 0.11. The other curve shows $|\psi|^2_{pot.-sprang}$, still for $E = \frac{1}{2}V_0$. This is the curve with the highest maximae for $x < 0$. (The reflection coefficient is 100 % for the potentila step). For $x > 0$ this curve has the form $|C|^2 e^{-2\kappa x}$ and goes to zero for large x. This curve is therefore *not* flat for $x = L$. Since $|\psi_{II}|^2 = |ae^{-\kappa x} + be^{\kappa x}|^2$ for the tunneling case is flat for $x = L$, we realize that ψ_{II} must contain a certain part of the increasing function $e^{\kappa x}$. However, because $e^{\kappa L}$ is much larger than $e^{-\kappa L}$, we do not need much of this function; from (T3.69) it follows that $|b/a| = e^{-2\kappa L}$. This is the reason why the two curves resemble each other so much in region II. We may conclude that estimates of T based on $|\psi|^2_{\text{pot.}-\text{sprang}}$ gives us the all-important factor $e^{-2\kappa L}$; we loose only the prefactor.

More realistic barriers

How large barriers are we talking about? To get an idea about the order of magnitude, we may assume that the particles are electrons and that V_0 is 1/4 Rydberg, that is,

$$V_0 = \frac{1}{4}\frac{\hbar^2}{2m_e a_0^2} = \frac{1}{4}\cdot 13.6\,\text{eV} \approx 3.4\ \text{eV}.$$

This gives

$$\gamma \equiv \sqrt{\frac{2m_e V_0 L^2}{\hbar^2}} = \sqrt{\frac{L^2}{4a_0^2}} = \frac{L}{2a_0}.$$

In this case, we obtain a barrier strength $\gamma = 2.5$ (as in the figure above) by choosing $L = 5a_0$, where a_0 is the Bohr radius. If we choose $E = \frac{1}{2}V_0 = 1.7$ eV, we have

$$\kappa L = L\sqrt{2m_e(V_0 - E)/\hbar^2} = \gamma/\sqrt{2},$$

so that the penetration depth becomes

$$l_{\text{p.d.}} = \frac{1}{2\kappa} = \frac{L}{\gamma\sqrt{2}} = a_0\sqrt{2}.$$

For this barrier we found a transmission probability 0.11.

In practice, the barriers are often much larger and T much smaller than in this example. T then becomes very sensitive to κL. If e.g. $T \sim e^{-2\kappa L} = 10^{-10}$, then a doubling of L gives a T of the order of 10^{-20}!

What about more realistic barriers, which do not have the idealized "square" form?

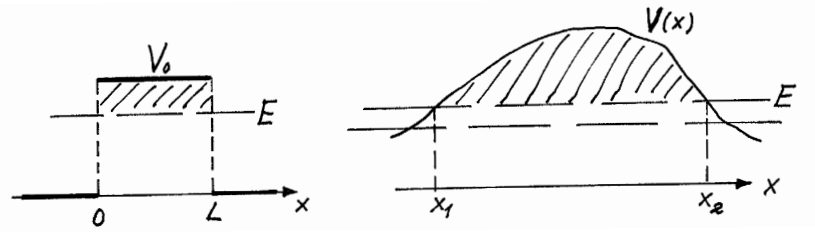

By taking the logarithm of the transmission coefficient (T3.80) for the square barrier and using that $L = \int_0^L dx$, we may write this logarithm in the following manner:

$$\ln T_{\text{tunn}} = \ln(\text{prefactor}) - 2\kappa L = \ln(\text{prefactor}) - \frac{2}{\hbar}\int_0^L \sqrt{2m(V_0 - E)}\,dx.$$

It is then tempting to ask if the formula

$$\ln T_{\text{tunn}} = \ln(\text{prefactor}) - \frac{2}{\hbar}\int_0^L \sqrt{2m[V(x)-E]}\,dx, \tag{T3.81}$$

where we have replaced V_0 by $V(x)$, will work for the more realistic potential on the right? The answer turns out to be yes. In chapter 8 Griffiths shows that this formula is correct, with a prefactor of the order of 1. (See also 8.4 in B&J.)

If this logarithm is a large negative number, we understand from the figure on the right that the logarithm will change drastically even for small changes of the energy E. In such cases the tunneling probability becomes very sensitive to small changes in the energy. This will be demonstrated for a couple of examples.

3.6.g Field emission

(Hemmer p 64, B&J p 420)

Tunneling plays an important role in many physical phenomena. One of these is **field emission**. In a metal at room temperature almost all electrons need a few extra electron volts in order to escape from the metal. This is the so-called work function which is well known from the discussion of the photoelectric effect, and which is typically of the order of $W \sim 2-5$ eV, depending on the type of metal, whether the surface is oxidized etc. On its way out through the metal surface, the electrons thus meet a potential step, and the deficit W in kinetic energy makes the outside a forbidden region with $\kappa = \sqrt{2m_e(V_0-E)/\hbar^2} \approx \sqrt{2m_eW/\hbar^2}$, and a penetration depth of the order of

$$l_{\text{p.d.}} = \frac{1}{2\kappa} = \tfrac{1}{2}\sqrt{\frac{\hbar^2}{2m_eW}} = \tfrac{1}{2}a_0\sqrt{\frac{\hbar^2}{2m_ea_0^2}\frac{1}{W}} \sim \tfrac{1}{2}a_0\sqrt{\frac{13.6}{4}} \sim 0.4\ \text{Å},$$

if we set $W = 4$ eV.

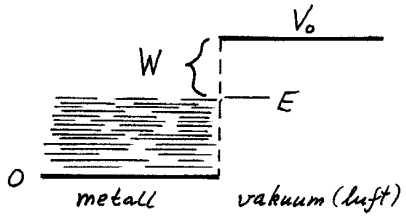

One way to liberate electrons is to radiate the surface with ultraviolet light (the photoelectric effect). An alternative is the "hot cathode" (or incandescent cathode), where electrons are "evaporated" by heating the metal to a sufficiently high temperature (cf the hot cathode in the old television tube). However, electrons can also be extracted from a "cold" cathode, using so-called **field emission**:

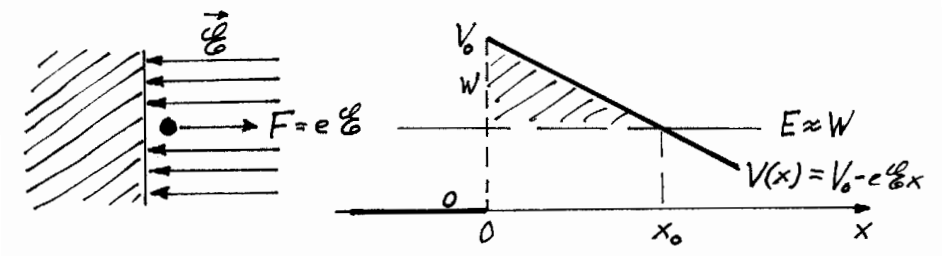

By exposing the metal for a strong electric field $\mathcal{E}$, we change the potential encountered by the electron from a step potential with $V_0 - E = W$ to a potential of the type $V(x) = V_0 - e\mathcal{E}x$. Here we are assuming a homogeneous $\mathcal{E}$-field. As shown in the figure, the electon now encounters a forbidden triangular barrier, where $V(x) - E = W - e\mathcal{E}x$, so that the length of the forbidden barrier is

$$x_0 = \frac{W}{e\mathcal{E}}.$$

From the penetration depth calculated above, we realize that x_0 must be made very small (of the order of Angstroms) in order to obtain a transmission probability that is not extremely small. This requires a very strong $\mathcal{E}$-field, $\mathcal{E} \sim \frac{W}{ex_0} \sim 10^{11}$ V/m, of the same order of magnitude as those found inside atoms. In practice, one is forced to work with weaker fields and correspondingly wider barriers. This gives very small values for T, but the field emission is still measurable and significant.

With the assumption of a homogeneous $\mathcal{E}$-field and hence with a triangular barrier, we must expect that $\ln T$ is proportional to the barrier length x_0, i.e. inversely proportional to $\mathcal{E}$. This can be verified by equation (T3.40), which gives

$$\begin{aligned}
\ln \frac{T}{\text{prefactor}} &= -\frac{2}{\hbar}\int_0^{x_0} \sqrt{2m_e[V(x)-E]}\,dx = -\frac{2\sqrt{2m_e}}{\hbar}\int_0^{x_0}\sqrt{W - e\mathcal{E}x}\,dx \\
&= -\frac{2\sqrt{2m_e}}{\hbar}\,\frac{W^{3/2}}{e\mathcal{E}}\underbrace{\int_0^1 \sqrt{1-y}\,dy}_{2/3} \qquad (y = \frac{e\mathcal{E}}{W}\,x) \\
&= -\frac{4\sqrt{2m_e}\,W^{3/2}}{3\hbar e}\,\frac{1}{\mathcal{E}}. \qquad \text{(T3.82)}
\end{aligned}$$

A typical work function for metals is $W \sim 4$ eV. With $m_e = 0.511$ MeV/c^2 for the electron and $\hbar = 0.6582 \cdot 10^{-15}$ eVs, we may then express the result as follows:

$$\ln \frac{T}{\text{prefactor}} \approx -54.6 \left(\frac{10^9 \text{ V/m}}{\mathcal{E}}\right)\left(\frac{W}{4 \text{ eV}}\right)^{3/2}. \qquad \text{(T3.83)}$$

Thus a work function of $W = 4$ eV and a field strength $\mathcal{E} = 10^9$ V/m gives $\ln T \approx -54.6$. Here, we have discarded the logarithm of the prefactor, which is unimportant in this connection.

Here it should be noticed that even if the transmission probability T is very small, we may get measurable field-emission currents, because of the large number of electrons which are colliding with the surface per second. [In the metal we have $\sim 10^{22}$ conduction electrons per cm^3, and with kinetic energies of the order of 5 eV these are moving with a velocity which is 1/200 of the velocity of light.]

It is also important to note that a moderate change of $V_0 - E$ or of $\mathcal{E}$ can change T by several "orders of magnitude" (powers of 10). As an example, if we reduce $\mathcal{E}$ from 10^9 V/m to $\frac{1}{2}\cdot 10^9$ V/m, this corresponds to a doubling of $\ln T$, from -54.6 to -109.2. The transmission probability then changes from $\sim 10^{-24}$ to $\sim 10^{-48}$.

Thus, as we have stressed before, the probability T is extremely sensitive to small changes in the length or height of the barrier. This property is exploited in modern applications of field emission, e.g. in **S**canning **T**unneling **M**icroscopy, STM. In STM, one uses escaped electrons to create a picture of the surface of the emitter.

3.6.h Scanning tunneling microscopy (STM)

(Hemmer p 65, B&J p 153)

In the STM microscope, the barrier is made up of the gap between e.g. a metal surface and the tip of a probe formed as a needle. By the use of a cleverly designed electro-mechanical system (including the use of piezo-electric forces) the tip can be brought very close to the surface. When a voltage is applied over the gap, a weak tunneling current will flow, as shown in the figure. This current is very sensitive to changes in the gap distance and hence to the structure of the surface. There are two ways to operate such a system:

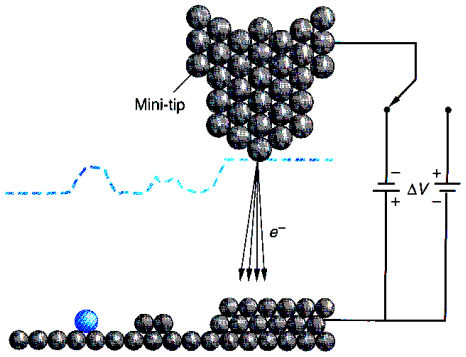

(i) In the **constant-current mode** a feedback mechanism is used to keep the distance between the probe (and hence also the current) constant. Then, under the sideways sweeping over the surface, the needle also is moved vertically, to keep the distance constant. By monitoring the vertical motion during a systematic sweeping we then get a picture of the surface; the needle follows the "mountains and the valleys" of the surface, or to be more specific, of the electron density of the surface atoms. The vertical resolution in such a microscope can be as small as 0.01 Å.

(ii) In the **constant-height mode**, the needle is sweeping along the surface at constant height, i.e., without vertical motion, and with a constant voltage over the gap. The current then will vary strongly following the variations in the distance from the needle to the surface. From these variations one can extract information on the topography of the surface.

The picture below is from a graphite surface,

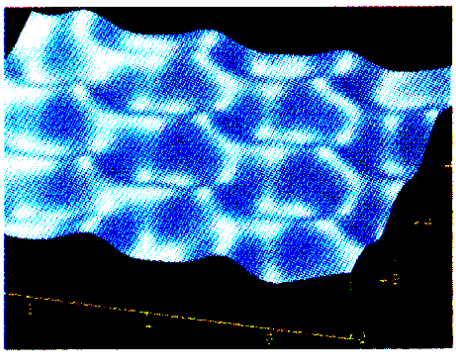

and clearly shows the ring structure of the top graphite layer. Each of the rings contains six carbon atoms, of which three seem to be lying slightly higher than the others. In reality, the six carbon *nuclei* lie in the same plane. The three atoms which seem to be lying lower than the others form bindings with atoms of the next layer immediately below them. Therefore

these binding orbitals are shifted a little downwards, compared with the orbitals of the atoms which do not have neighbours right below them. [17] It is these differences in the eletron density which are monitored by this method.

3.6.i α decay and fusion

(Hemmer p 65, B&J p 421, Griffiths p 281)

A long time before tunneling was applied in technology it was discovered that the process plys an important role in several natural phenomena. One of these is α-**decay**, where heavy radioactive nuclei decay emitting α particles (helium nuclei).

It turns out that nuclei with $Z \geq 84$ and nucleon number $A(= Z + N) \geq 210$ are all more or less unstable and decay mainly via emission of α particles. The experimental lifetimes τ (and the half-lives $\tau_{1/2}$) for such α emitters show extreme variations — from extremely unstable ones like e.g. ${}^{212}_{84}$Po with a lifetime of less than a microsecond — and all the way up to almost stable nuclei with lifetimes of the order of the age of the universe, $\sim 10^{10}$ years, which occurs e.g. for ${}^{238}_{92}$U. This is a span of around 25 orders of magnitude.

The strange thing is that these lifetimes are also strongly correlated with the kinetic energies of the emitted α particles. The kinetic energies are largest for the most short-lived nuclei — up to $\sim$ 9 MeV — and smallest for the most stable ones — down to 4 MeV. Lower kinetic energies than $\sim$ 4 MeV are not observed for emitted α particles.

Already in 1928, soon after quantum mechanics was discovered, George Gamow (and independently, R.W. Gurney and E.U. Condon) proposed tunneling as an explanation of α decay. Gamow's explanation is easy to understand when one considers the potential $V(r)$ between the α particle with charge $2e$ and the remaining nucleus — often called the **daughter nucleus** — with charge Ze. When the distance r is a little larger than the radius r_1 of the "daughter", V is is a pure Coulomb potential,

$$V(r) = \frac{2Ze^2}{4\pi\epsilon_0}\,\frac{1}{r} \qquad\qquad (r \gtrsim r_1).$$

For $r \lesssim r_1$, this potential is modified due to the finite size of the proton distribution, and even more important, due to the **strong nuclear force**, which is the force that keeps the nuclei together, in spite of the Coulomb repulsion between the protons. The strong force has a very short range ($\sim$ 1 fm). In our simple model this means that the α particle is strongly attracted by the "daughter" when being close to the surface. This leads to a total interaction potential between the α particle and the daughter with the following (somewhat simplified) form:

[17] The scanning tunneling microscope has a serious drawback; it requires a surface that is electrically conducting. Alternatively, a non-conducting surface has to be covered by a layer of conducting atoms. This is a problem also for metals like aluminum, where the surface is covered by non-conducting oxides. In the AFM microscope (**A**tomic **F**orce **M**icroscope) one avoids this problem by using a probe made from cheramics or some semiconducting material. During sweeping, this probe is kept pressed aganst the surface by a weak force. This force is balanced by a repusive force due to the Pauli principle (which attempts to keep the electron clouds in the needle and the surface separated from each other). Here, the needle is moving vertically much the same way as in the constant-current-mode above. An AFM microscope can also work in **non-contact mode**, where the topography is monitored by a probe kept at a certain distance from the specimen.

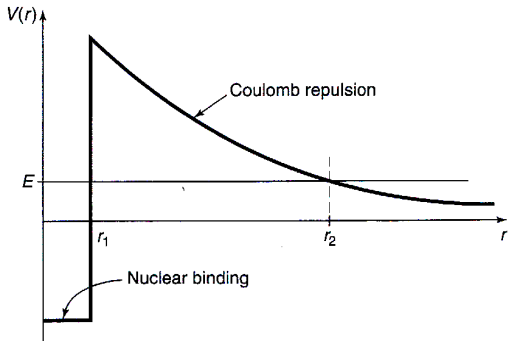

The radius r_1 of the daughter can empirically be taken to be

$$r_1 \approx (1.07 \text{ fm}) \cdot A^{1/3}, \tag{T3.84}$$

which is $r_1 \sim 6 - 7$ fm for $A \sim 210$ ($Z \sim 80$). This means that the "height" of the Coulomb barrier is approximately

$$V(r_1) = \frac{2Ze^2}{4\pi\epsilon_0}\frac{1}{r_1} \sim 30 \text{ MeV}.$$

As illustrated in the figure, this maximum is much higher than the energy E of the emitted α particle. Classically, the α-particle can therefore not escape, even though its energy is positive. However, according to quantum mechanics there is a small chance that it may tunnel through the Coulomb barrier each time it hits the surface from the inside of the nucleus. This means that the state of the α particle is not really a truly stationary bound state, but what we often call a metastable state. To get an idea about how many chances the particle gets to escape, we may use a simplified semiclassical argument: We assume that the particle is moving back and forth between the "walls" of the nucleus with a velocity which is of the order of $\sqrt{2E/m_\alpha}$. This gives an impressive collision rate (number of collisions per unit time)

$$\nu \sim \frac{v}{2r_1} \sim \frac{c}{2r_1}\sqrt{\frac{2E}{m_\alpha c^2}} \sim 10^{21} \text{ s}^{-1}.$$

Although this estimate is semiclassical and very rude, we understand that the transmission coefficients must be very small; otherwise the lifetimes ($\tau = 1/(\nu T)$) would indeed be very short. This means that

$$\ln T \approx -\frac{2}{\hbar}\int_{r_1}^{r_2} \sqrt{2m_\alpha[V(r) - E]}\, dr$$

for these Coulomb barriers must be large negative numbers; we are dealing with almost impenetrable barriers. Then without actually doing any calculations, we can state that the difference between the logarithms $\ln T$ for $E \approx 9$ MeV and $E \approx 4$ MeV, will be large, cf the figure. This way we can understand why the lifetimes vary with as much as 25 powers of 10.

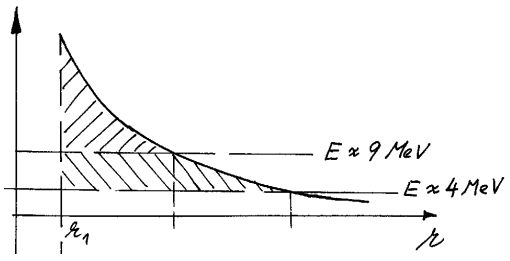

From this argument we can also understand why α radioactivity with $E \lesssim 4$ MeV is not observed. This is because for α particles with lower energies, the barrier is so large that it is in practice impenetrable. The lifetimes then become larger than 10^{10} years, and such nuclei are in practice stable.

These considerations also illustrate why it so difficult to obtain *fusion* of nuclei under laboratory conditions. Even with temperatures of the order of $1.5 \cdot 10^7$ K, which are found in the core of the sun, the thermal kinetic energy of the nuclei is as small as $\frac{3}{2}k_BT \sim 1$ keV. With kinetic energies of this size, it becomes extremely difficult for two nuclei to overcome the Coulomb barrier, so that they get close enough to merge into a heavier nucleus. However, there still is a small chance for tunneling so that fusion can take place, and it is processes of this kind that keeps the sun burning.